

EXPLOSIONS IN WOLF-RAYET STARS AND TYPE Ib SUPERNOVAE. I. LIGHT CURVES<sup>1</sup>

LISA M. ENSMAN AND S. E. WOOSLEY

Board of Studies in Astronomy and Astrophysics, Lick Observatory, University of California at Santa Cruz

Received 1988 March 7; accepted 1988 April 20

## ABSTRACT

Numerical models of core-bounce supernovae with hydrogenless "Wolf-Rayet" progenitors are presented. The luminosity near peak light of these supernovae is provided by the escape of radioactive decay energy which accumulates in the optically thick interior and diffuses outward until it meets the inwardly moving photosphere (recombination front). It has been suggested that such stars are the source of Type Ib supernovae. Type Ib peak magnitudes and light curves have been collected from the literature, analyzed, and compared with the models. We find that the models have difficulty matching the observed decline in luminosity immediately after peak in SN 1983N, the prototypical Type Ib supernova (SNIb). However, they may be able to fit the light curve of the unusual SNIb 1985F. If some or all Type Ib progenitors are Wolf-Rayet-like stars, the widths of the supernova light curves constrain them to be between about 4 and 7  $M_{\odot}$ , originally 15–25  $M_{\odot}$  on the main sequence.

*Subject headings:* stars: interiors — stars: supernovae — stars: Wolf-Rayet

## I. INTRODUCTION

Supernovae fall into two general classes: Type I (SNI), which do not have hydrogen in their spectra, and Type II (SNII), which do (Minkowski 1941). The Type II's can be further divided into two subgroups (Barbon, Ciatti, and Rosino 1979): SNII-P, which have a plateau phase in their light curve, and SNII-L, which decline linearly from peak. Even within these subgroups, there is considerable variation in brightness, light curve, and spectrum. Type I supernovae, on the other hand, have traditionally formed a much more homogeneous class, but recent observations of SN 1983N and SN 1984L have resulted in the identification of a distinct new subclass, Type Ib. While theorists have generally linked classical Type I supernovae (henceforth SNIa) to exploding white dwarfs (see Woosley and Weaver 1986 for a review), the origin of Type Ib (SNIb) supernovae remains controversial (Wheeler and Levreault 1985; Chevalier 1986; Cameron and Iben 1986; Branch and Nomoto 1986; Uomoto 1986; Khokhlov and Ergma 1986; Iben *et al.* 1987; Branch 1988). Their progenitors could be white dwarfs or other hydrogen-deficient objects, the most popular speculation in recent years being that they are "Wolf-Rayet" stars, massive stars which have completely lost their hydrogen envelopes before dying. Following a brief review of the observations and previous theoretical work, this paper will examine the massive-star hypothesis by comparing model light curves with observed Type Ib light curves. A second paper in this series (Woosley and Weaver 1988) will describe in more detail the presupernova stars and the explosions, nucleosynthesis, and dynamics of the models. Paper III (Pinto, Axelrod, and Woosley 1988) will examine constraints provided by spectra (see also Axelrod 1988).

## II. TYPE Ib SUPERNOVAE

## a) Observations

The Type Ib class of supernovae was first recognized as a distinct subtype in the early 1980s (Elias *et al.* 1985; Wheeler and Levreault 1985), after the events SN 1983N and 1984L,

which were seen to resemble the spectroscopically peculiar SN 1962L (Bertola 1964) and 1964L (Bertola, Mammano, and Perinotto 1965). Several other Type Ib supernovae (SNIb) have since been identified, including SN 1985F, the Filippenko-Sargent object (Filippenko and Sargent 1985), SN 1983I, 1982R, and perhaps 1954A, 1975B, 1983V, and 1986M (Chevalier 1986; Gaskell *et al.* 1986; Graham 1986a and references therein; Elias *et al.* 1985; Wheeler, Harkness, and Cappellaro 1987). Most of the characteristics of Type Ib supernovae are inferred from a rather sparse data set; few SNIb have been discovered, and none have been observed continuously at all wavelengths. Porter and Filippenko (1987) give a good summary of the observations of individual SNIb.

As will be discussed in greater detail below, except for the fact that SNIb are 1.5–2 mag dimmer than SNIa *on average* in the *blue*, SNIb light curves are nearly indistinguishable from those of SNIa. The greatest differences can be found in the spectra, although there are interesting similarities as well. The class is defined spectroscopically (e.g., Porter and Filippenko 1987): SNIb lack, in addition to hydrogen, an absorption feature near 6150 Å, the blueshifted absorption trough of a P Cygni profile produced by a blend of Si II  $\lambda\lambda 6347, 6371$ . This feature is prominent in Type Ia spectra until it disappears about a month after peak light. Probably the most dramatic difference between SNIb and other supernovae is the late-time spectrum (e.g., SN 1984L at 400 days past peak: Kirshner, cited in Chevalier 1986; 1983N at 226 days: Gaskell *et al.* 1986; 1985F; Filippenko and Sargent 1985). In the optically thin "supernova" phase beginning a few hundred days after peak light, SNIb spectra are dominated by [O I]  $\lambda 6300$  rather than by iron peak elements, as in SNIa, or H $\alpha$ , as in SNII. See also Branch and Nomoto (1986), Pinto (1988), and Filippenko and Sargent (1985) for other late-time spectral characteristics.

At earlier times, Type Ia and Type Ib spectra are broadly similar. The closest resemblance is between SNIb (before) at peak and SNIa (at) 20 days to 2 months after peak (Branch *et al.* 1983, 1985; Harkness 1987; Wheeler and Levreault 1985; Harkness *et al.* 1987; Blair and Panagia 1987; Panagia 1987; Richtler and Sadler 1983; Uomoto and Kirshner 1985). By analogy, then, the photosphere in SNIb must lie in material

<sup>1</sup> Lick Observatory Bulletin, No. 1110.

composed of intermediate elements before maximum and in iron by peak (Wheeler and Levreault 1985). This interpretation may prove to be too simplistic, however. Many of the deep absorption features seen in Type Ib spectra at maximum can be attributed to helium rather than iron (Wheeler and Harkness 1986; Branch and Nomoto 1986). Wheeler *et al.* (1986) speculate that there may be a sequence of different helium masses within the Type Ib class. Harkness *et al.* (1987) have thrown even more doubt on the notion that there is a large fraction of iron in the outer layers of SNIb by constructing a model atmosphere consisting predominantly of helium (very much out of LTE), with only *solar* abundances of iron, which matches the spectra fairly well.

At late times, after the ejecta has thinned sufficiently, more iron (presumably originally  $^{56}\text{Ni}$ ) can be seen. A year after peak, Graham *et al.* (1986) concluded from observations of the  $[\text{Fe II}]$  1.644  $\mu\text{m}$  line that  $0.3 \pm 0.2 M_{\odot}$  of iron was present in the remnant of SN 1983N, assuming a distance of 5 Mpc, about half that expected from a Type Ia. For  $d = 3.7$  Mpc, de Vaucouleurs's (1979) value (and that used in § Vd), the amount would be reduced to about  $0.17 M_{\odot}$ . The derivation assumed Axelrod's (1980) emissivity for an iron nebula, and the iron mass should be revised if  $[\text{O I}]$  dominates the cooling (Graham in Gaskell *et al.* 1986). Interestingly, the line was narrower than in SNIa, implying a lower expansion velocity in the core.

It is intriguing that all the SNIb observed so far have been found in spiral galaxies. For comparison, about three-fourths of SNI, in general, are discovered in spirals. (Correcting for the fact that we see more spiral galaxies than ellipticals, one can estimate that only about 28% of SNI actually occur in spirals; Barbon, Ciatti, and Rosino 1973.) Further, all the Type Ib's have been found very near or coincident with H II regions and/or spiral arms, classic Population I environments (Richter and Rosa 1984; Wheeler and Levreault 1985; Filippenko and Sargent 1985; Porter and Filippenko 1987).

SNIb also appear to have unique characteristics in the infrared (Elias *et al.* 1985), and at least two have been seen in the radio near peak light (Sramek, Panagia, and Weiler 1984; Panagia, Sramek, and Weiler 1986). Radio emission is normally associated with interaction between the ejecta and circumstellar matter of some sort (Chevalier 1984, 1986). No other Type I supernovae have ever been detected at radio wavelengths (Sramek, Panagia, and Weiler 1984); and although Type II supernovae are known to emit in the radio, they do not resemble the Type Ib's which peak sooner and decay faster (Sramek, Panagia, and Weiler 1984; Porter and Filippenko 1987; Weiler *et al.* 1986). The differences between Type Ia and Type Ib infrared light curves may be related to the abundance of silicon (Graham 1986a; Wheeler and Levreault 1985).

It has often been said (e.g., Porter and Filippenko 1987; Uomoto and Kirshner 1985) that, neglecting differences in luminosity, the optical light curves of SNIb and SNIa are nearly identical in shape. Although the data are sparse, it is clear from comparisons shown in Figure 1 that this is not true for SN 1985F and is true for the other SNIb only during the first few months. Figure 1a shows the blue light curves of SNIb, taken from the literature, and Figure 1b shows the visual and bolometric data. Figure 1c shows the blue data on a longer time scale. These figures were constructed by requiring that the light curves coincide at peak. In the case of 1983I, the data were shifted both horizontally and vertically to obtain the best fit to the mean type Ia curve. (The placement shown corre-

sponds to peak  $B = 14$  on JD 2,445,454 and  $V = 13.7$  on JD 2,445,455; the peak absolute magnitudes implied are consistent with those of the other SNIb.) The mean SNIa  $B$ -magnitude (actually blue and photographic) light curve is based on a sample of 38 Type I supernovae, which included two SNIb. The  $V$ -magnitude light curve is based on only three SNIa (Doggett and Branch 1985) and should have more curvature between 0 and 50 days.

These figures highlight several interesting points. First, on the scale of Figures 1a and 1b, the light curves of SNIb do indeed appear to be identical with those of SNIa, with the exception of SN 1985F. Note, however, that in the visual band both types are broader and have less pronounced peaks. The shape of the bolometric light curve of SN 1983N (Blair and Panagia 1987; Panagia 1987) is also shown in Figure 1b. Since most of the emission is in the visual at all epochs, the bolometric light curve closely follows the  $V$ -magnitude curve but not the  $B$ . It should be stressed that much (including some of the major conclusions of this paper) depends on the accuracy of the last two data points. Good bolometric observations of future SNIb are *essential* for confirming the validity of many of the statements we shall make.

In Figure 1c it becomes apparent that SNIa decline more quickly on the tail. Panagia, as cited in Wheeler and Harkness (1986), also states that SNIb decay more slowly at "late times." Since supernovae are powered by radioactive decay on their tails, this implies that Type Ia's are becoming transparent to the gamma rays faster (see Weaver, Axelrod, and Woosley 1980). Although there are too few points to unambiguously define the tail of SN 1985F, a slope parallel to that of 1964L is consistent with the data. Interestingly, the dashed lines have a slope of 0.01 mag per day, the same decay rate as  $^{56}\text{Co}$ .

SN 1985F, the Filippenko-Sargent object, may not have been an ordinary Type Ib supernova. It was discovered during the late supernova phase and appeared, at first, to be unlike any previously observed supernova (Filippenko and Sargent 1985, 1986). Later, unpublished late-time spectra of SN 1984L and SN 1983N were found to have a very similar appearance (Kirshner, cited in Chevalier 1986; Gaskell *et al.* 1986). On the basis of this similarity, SN 1985F was identified as a Type Ib supernova discovered 8 months or so past maximum. The first manifestation of its unusual nature occurred when, contrary to expectation, it was not detected in the radio (Sramek 1985, quoted in Filippenko *et al.* 1986). Chevalier (1986) and Filippenko *et al.* (1986) concluded that something must be odd about either its radio properties, its optical light curve, or its estimated age. Perhaps, as in SN 1987A, the circumstellar density around SN 1985F was particularly low. The age determination has since been confirmed by the publication of photometric observations near peak light (Tsvetkov 1986), but, as shown in Figure 1, the light curve is indeed somewhat unusual. It was broader and faded less immediately after peak than did those of the other Type Ib's. Unfortunately, no spectra were taken near peak light, so the identification of SN 1985F as a Type Ib must remain circumstantial.

#### b) Theory

The locations of SNIb, their lack of hydrogen but wealth of oxygen, their faint light curves and radio emission, all point toward relatively compact and hydrogenless massive progenitors, i.e., Wolf-Rayet stars (e.g., Chevalier 1976; Maeder and Lequeux 1982). On the other hand, the close similarity of Type Ia and Type Ib light curves and spectra suggests a white dwarf

precursor as in SNIa. Wheeler and Levreault (1985) discussed the possibilities and concluded that SNIb progenitors, which could not have a total mass much in excess of  $3 M_{\odot}$ , should undergo core collapse and bounce, like SNII, but have light curves dominated by the decay of  $^{56}\text{Ni}$  made in the explosion, like SNIa.

To test such speculation, we began to compute numerical models of Wolf-Rayet stars which undergo iron core collapse and produce "core-bounce" supernovae. Stars over about  $100 M_{\odot}$  will collapse as a result of the pair instability during oxygen burning. They are not of interest here, since, if they do produce supernova explosions, their light curves will be extremely broad. Another group, Cahen, Schaeffer, and Casse (1986), extended Arnett's (1980, 1982) analytical approach to include the energy released by recombination and applied it to two Wolf-Rayet models. The light curves they first derived were dominated by the energy released by the recombination of oxygen. Although they noted its importance, they did not include significant amounts of radioactive nickel in their calculations. As our early numerical models showed (Woosley 1986), radioactive decay is entirely responsible for the peaks in the light curves of core-bounce supernovae without hydrogen.

Once they included a few tenths of a solar mass of nickel (Schaeffer, Casse, and Cahen 1987), their light curves changed considerably and the shape of the lighter one (an  $8 M_{\odot}$  core-bounce model) now agrees quite well with our numerical models 8B and 6C described in § IV (assuming that the bolometric light curve is very similar to the visual band light curve that they give). However, to make the match, one needs to shift the time of peak. Their premaximum display (§ IV) lasts much longer than ours does, hence the peak occurs later than in our models. It is not certain how important this is; it is probably a result of differences in the density structure and the exact composition and opacities used. (Their  $8 M_{\odot}$  star came from a  $40 M_{\odot}$  star, while ours was originally only  $25 M_{\odot}$ ; and they may have removed the helium layer which we kept.) Or the difference may be the result of different physics and approximations inherent in the use of analytical as opposed to numerical methods.

### III. NUMERICAL TECHNIQUES AND ASSUMPTIONS

We have employed the stellar evolution/explosion code KEPLER (Weaver, Zimmerman, and Woosley 1978; Weaver, Woosley, and Fuller 1985) to follow the evolution of several

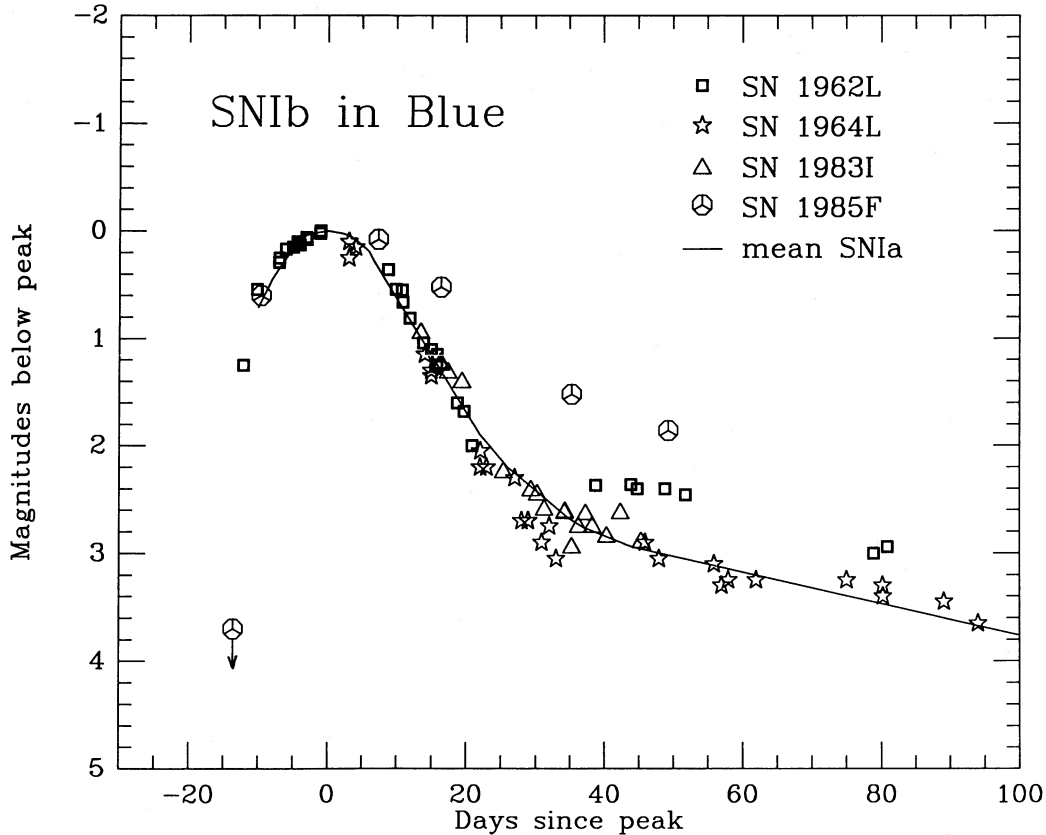


FIG. 1a

FIG. 1.—(a) Normalized blue magnitude light curves for observed Type Ib supernovae. (The SN 1964L data are actually  $m_{pk}$ .) The solid line shows the mean *B* light curve of Type Ia supernovae. On the scale shown, SNIa and SNIb are nearly identical, with the exception of SN 1985F. Sources: Bertola (1964); Bertola, Mammano, and Perinotto (1965); Tsvetkov (1985, 1986); Doggett and Branch (1985). (b) Normalized *V*-magnitude and bolometric light curves for observed Type Ib supernovae. The *V* light curve of SN 1983N was obtained using the Fine Error Sensor of IUE, and the bolometric curve was obtained by direct integration of spectra. The solid line shows the mean *V* light curve of Type Ia supernovae. It is based on only three SNI and should probably have more curvature between 10 and 40 days. The dashed line is the mean SNIa *B* light curve. Again, the light curves of SNIa and SNIb are seen to be nearly identical in shape. The bolometric luminosity tracks the visual output, and both evolve differently than the blue magnitude. Sources: Bertola (1964); Tsvetkov (1985); Blair and Panagia (1987); Doggett and Branch (1985). (c) Blue light curves of observed Type Ib supernovae on an extended time scale. For comparison, the solid line shows the mean SNIa blue light curve. The dashed line through the SN 1985F data was chosen to have the same slope as that through the SN 1964L points, and both decay at the same rate as  $^{56}\text{Co}$ . This may be a coincidence, since the bolometric output does not appear to track the blue light curves (see [b]).

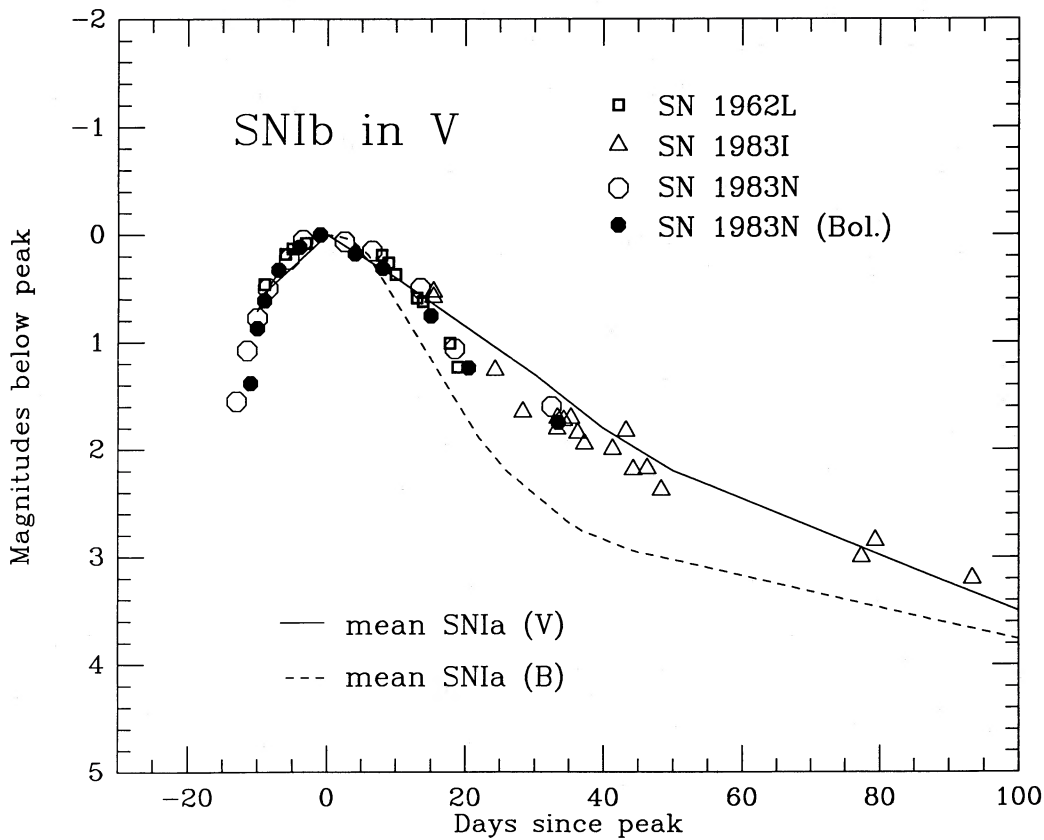


FIG. 1b

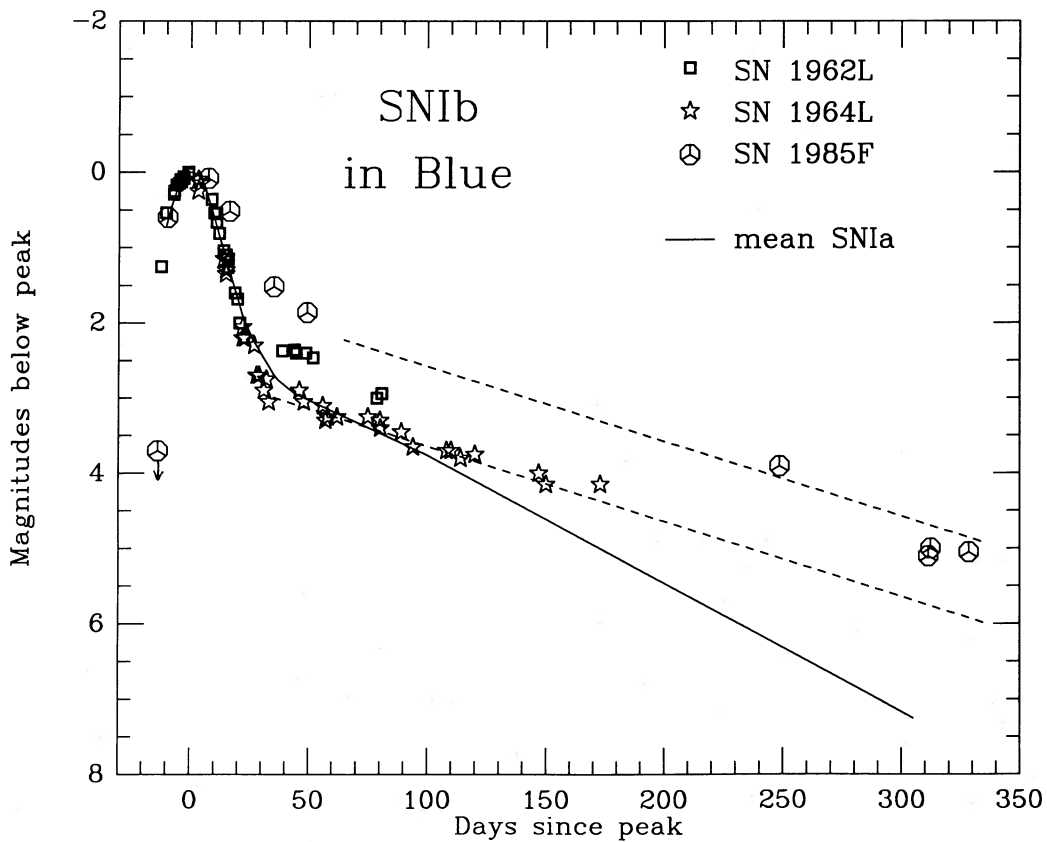


FIG. 1c

TABLE 1  
 MODEL PARAMETERS

PARAMETER	MODEL									
	4A	4B	6A	6B	6C	8A	8B	14A	14B	23A
Main-sequence mass ( $M_{\odot}$ )	15	15	20	20	20	25	25	35	35	50
Wolf-Rayet mass ( $M_{\odot}$ )	4.1	4.1	6.2	6.2	6.2	8.43	8.43	14.26	14.26	22.85
Total mass ejected ( $M_{\odot}$ )	2.68	2.68	4.50	4.50	4.50	5.98	5.98	12.41	12.41	20.37
Oxygen ejected ( $M_{\odot}$ )	0.4	0.4	1.3	1.2	1.3	2.6	2.4	6.4	6.5	11.6
Nickel ejected ( $M_{\odot}$ )	0.06	0.08	0.44	0.51	0.16	0.28	0.33	0.26	0.40	0.69
Explosion energy <sup>a</sup> ( $10^{51}$ ergs)	0.5	3.2	1.4	4.2	2.7	1.0	2.9	1.2	9.7	2.1
Peak $L_{\text{bol}}$ ( $10^{42}$ ergs $\text{s}^{-1}$ )	1.29	2.13	7.44	10.2	3.33	3.16	5.15	2.20	4.33	4.84
FWHM (days)	29	21	38	31	31	73	44	94	40	108
Fit to SN 1983N <sup>b</sup>	F	(F, E)	B	E, Ni	...	B	B	B, (F)	B, E	B

<sup>a</sup> Kinetic energy. Equal to total energy at late times.

<sup>b</sup> B = too broad; F = too faint; E = too energetic; Ni = too much  $^{56}\text{Ni}$ . Parentheses indicate quantities which are marginally too extreme. All models fail to match the postpeak decline of SN 1983N.

supernovae. This code includes implicit hydrodynamics, flux-limited (one-temperature) radiative diffusion, hydrostatic and explosive nucleosynthesis, local radioactive decay energy deposition, and opacity from electron scattering with a floor of  $10^{-3}$  (or  $10^{-4}$ )  $\text{cm}^2 \text{g}^{-1}$ . The floor opacity is used to simulate line and bound-free opacities which become important as the gas recombines. The code was modified for this study to calculate all ionization states of hydrogen, nitrogen, and the atoms with even nuclear charge up to  $^{56}\text{Ni}$  (assuming LTE) by iteratively solving a set of coupled Saha equations for the electron density.

Once its mass has been determined, the helium core of a massive star will evolve essentially independent of the hydrogen envelope, hence the final evolutionary stages and subsequent core collapse and bounce should be nearly the same in mass-losing stars as in those without mass loss (Chiosi and Maeder 1986). Previous studies have shown [for the current  $^{12}\text{C}(\alpha, \gamma)^{16}\text{O}$  reaction rate; Caughlan *et al.* 1985] that stars having main-sequence masses between about 10 and 65  $M_{\odot}$  ignite all six burning stages nondegenerately and undergo a core collapse triggered by photodisintegration and electron capture. Those less massive than about 20  $M_{\odot}$  (corresponding to helium core or Wolf-Rayet masses less than about 6  $M_{\odot}$ ) are believed to explode via a prompt hydrodynamical core bounce. More massive models require the still controversial neutrino-mediated delayed explosion process of Wilson (1985; Wilson *et al.* 1986). Regardless of how the explosion occurs, the results are essentially those produced by instantaneously depositing on the order of  $10^{51}$  ergs at the base of what will become the ejecta.

As will be described in greater detail in Paper II (see also Woosley 1986; Woosley, Pinto, and Ensmann 1988), explosions of W-R stars were modeled by removing the hydrogen envelopes from previously evolved stars (Wilson *et al.* 1986) soon after core collapse began. To avoid the complexities of explosion physics, the iron core, which would have collapsed to a neutron star, was also removed and replaced by a piston that could simulate core bounces of various energies. In most cases, models were run in pairs. The number in the model name refers to the progenitor mass and the letter to the explosion energy (i.e., the kinetic energy of the ejecta at infinity), version B being the more energetic. Note (Table 1) that the explosion energies of models 14B, 6B, 4B, and perhaps 8B,  $(2.9\text{--}9.7) \times 10^{51}$  ergs, are on the high side. For comparison, SN

1987A had an explosion energy between 0.5 and  $2 \times 10^{51}$  ergs (Woosley 1988).

Since neither mass loss nor the explosion was treated realistically in the calculations, the amount of mass removed from the surface and the core was somewhat arbitrary. The outer mass cut is constrained by the fact that helium but no hydrogen or oxygen has been identified in spectra of SNIb taken at early times, implying that the stellar surface is situated somewhere in the helium layer. The amount of mass removed from the core was guided by explosion calculations of Wilson *et al.* (1986) and other considerations described in Paper II, in particular, natural discontinuities in density, entropy, and composition. Stars with helium cores less massive than 4  $M_{\odot}$  were not considered because they create negligible amounts of radioactive  $^{56}\text{Ni}$  (Mayle and Wilson 1988) and produce very dim supernovae. The fraction of synthesized  $^{56}\text{Ni}$  ejected depends on the mass cut and is uncertain both theoretically and observationally. Model 6C was given a mass cut farther from the center of the star than in the other models, as would be the case if some matter outside the iron core had fallen onto the neutron star instead of being ejected. Larger mass cuts in other models were simulated by multiplying the radioactive energy release by a factor less than unity. This mimics with fair accuracy the actual ejection of a smaller fraction of the  $^{56}\text{Ni}$ . These models, named X-b (Table 2), are identical in all other respects to the corresponding models X in Table 1. Only in the case of SN 1987A is the mass of ejected  $^{56}\text{Ni}$  well known. That event ejected only 0.07  $M_{\odot}$  of nickel (Woosley 1988). A nickel

 TABLE 2  
 PARAMETERS FOR SECONDARY MODELS

PARAMETER	MODEL			
	6A-b	6B-b	6C-b	8A-b
Wolf-Rayet mass ( $M_{\odot}$ )	6.2	6.2	6.2	8.43
Effective nickel mass ( $M_{\odot}$ )	0.07	0.16	0.08	0.14
Explosion energy <sup>a</sup> ( $10^{51}$ ergs)	1.4	4.2	2.7	1.0
Peak $L_{\text{bol}}$ ( $10^{42}$ ergs $\text{s}^{-1}$ )	1.33	3.39	1.72	1.79
FWHM (days)	33	28	28	60
SN 1983N <sup>b</sup>	B, F	E	F	B, F

NOTE.—These models are variations of those in Table 1. Only the nickel mass was altered.

<sup>a</sup> Kinetic energy. Equal to total energy at late times.

<sup>b</sup> Notation as in Table 1.

mass of  $\sim 0.1 M_{\odot}$  has also been inferred for the Type II supernova SN 1980K (Uomoto and Kirshner 1986). Model 6A-b, plus about  $10 M_{\odot}$  of hydrogen envelope, would have produced a supernova like SN 1987A.

In this paper, the “bolometric” luminosity is taken to be the sum over all wavelengths of the thermal emission; unthermalized gamma rays and X-rays from radioactive decay are not included. Effects of the interaction between the ejecta and any circumstellar matter have not been included.

#### IV. LIGHT CURVES

The light curves of several models whose parameters are given in Tables 1 and 2 are shown in Figure 2. All the light curves have a characteristic premaximum display, followed by the main peak and an exponential tail. Shock breakout is not resolved on the scales shown, and poor surface zoning resulting from the artificial removal of the hydrogen envelope makes the models inaccurate during that period, so the spikes of hard radiation which accompany it are not always shown.

The composition and velocity of the ejecta are determined by the strength of the explosion. As the shock wave generated by the (simulated) core bounce propagates through the star, it raises the temperature and density enough in the inner layers to induce explosive nucleosynthesis. At the same time, it accelerates the material, expelling it at high velocity. More energetic explosions and less massive stars both give higher expansion velocities. After shock breakout, the ejecta expand homolo-

gously except for some acceleration of the innermost layers by radioactive decay energy (see Woosley 1988 and Paper II). Figure 3 shows the composition of the ejecta in three representative models. All have a characteristic layered composition consisting of an inner “core” of radioactive  $^{56}\text{Ni}$  topped by silicon, a massive oxygen layer, and an outer helium shell. No mixing during or after the explosion has been taken into account. Figure 4 shows the final velocity profiles. Acceleration of the inner layers by energy from radioactive decay has flattened the velocity gradient near the center. Finer zoning and a better initial density distribution at the surface would give even higher velocities to decreasing amounts of helium.

Model 8A will be described in some detail to show the sequence of events that occur as these supernovae evolve. Time points referred to are labeled on the light curve in Figure 5 and are also given in Table 3. As can be seen from Figure 6a, the premaximum peak in the light curve, which covers the period  $t1$  to  $t9$ , occurs during the recombination of the helium layer. At shock breakout, the helium is completely ionized; by  $t4$  it is only singly ionized. From  $t4$  to  $t9$  a “recombination front” eats its way through the helium layer. While the opacity due to electron scattering drops a little as each electron is captured by the highly ionized atom, it is the dramatic drop in the electron density by orders of magnitude as the dominant element becomes neutral at the recombination front which is important to the light curve. The logarithm of the opacity ( $\text{cm}^2 \text{g}^{-1}$ ) falls from  $\sim -1$  to  $\sim -2.5$  across the front. Figure 7 shows the

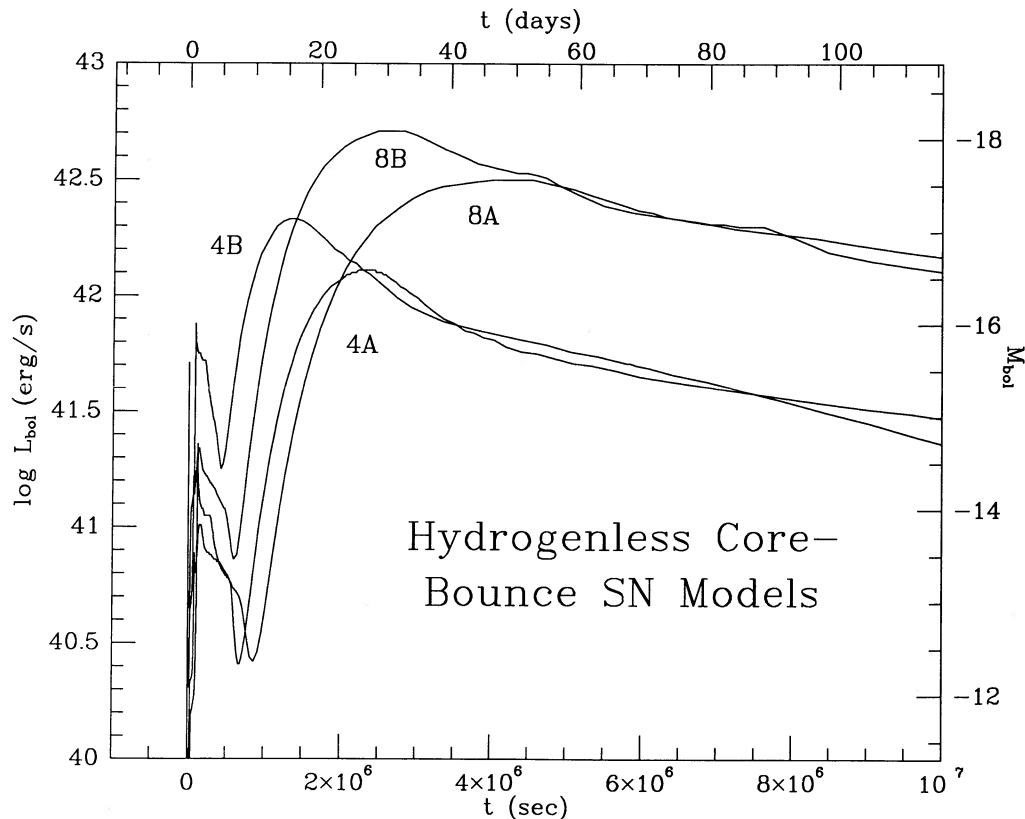


FIG. 2a

FIG. 2.—(a) Bolometric light curves of models with 4 and  $8 M_{\odot}$  “Wolf-Rayet” progenitors. In each pair, version B was given a more powerful explosion than version A. (b) Bolometric light curves of models with  $6 M_{\odot}$  progenitors. Model 6C has an explosion of intermediate strength, but it ejected less radioactive  $^{56}\text{Ni}$  than either model 6A or model 6B. Model 6A-b was identical to model 6A, except that it ejected a sixth as much  $^{56}\text{Ni}$ . It would have been very like SN 1987A if it had had a hydrogen envelope. (c) Bolometric light curves of models with 14 and  $23 M_{\odot}$  progenitors. Note the change in scale relative to (a) and (b).

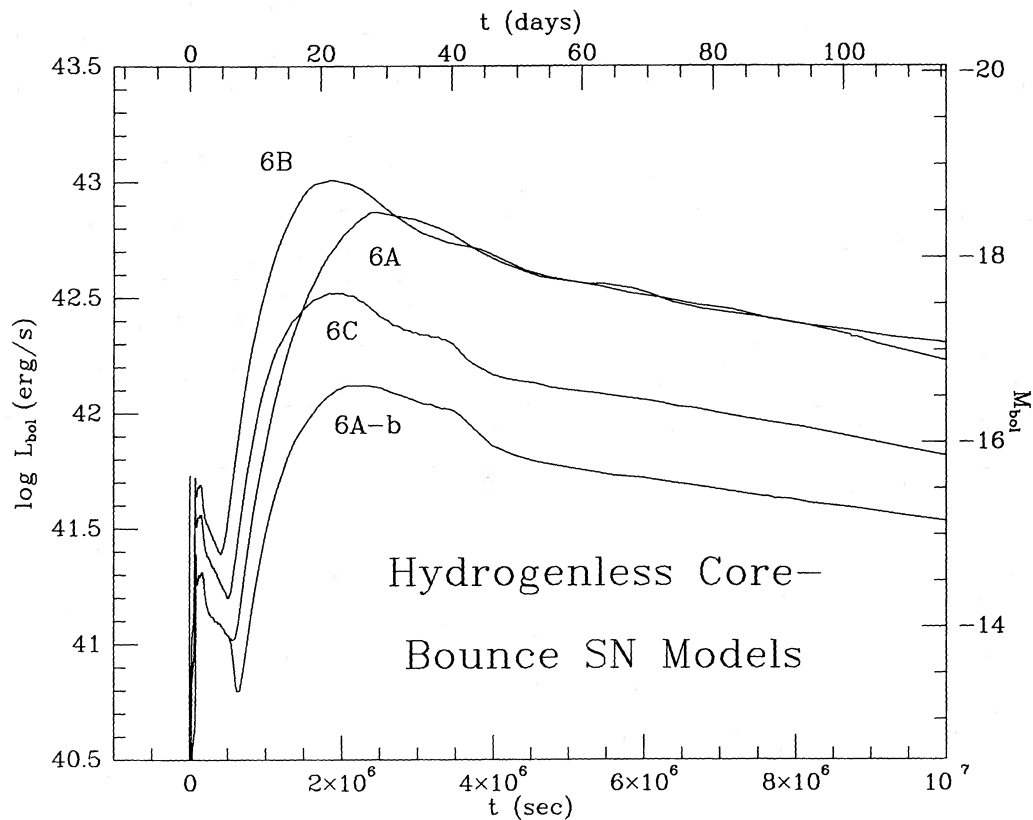


FIG. 2b

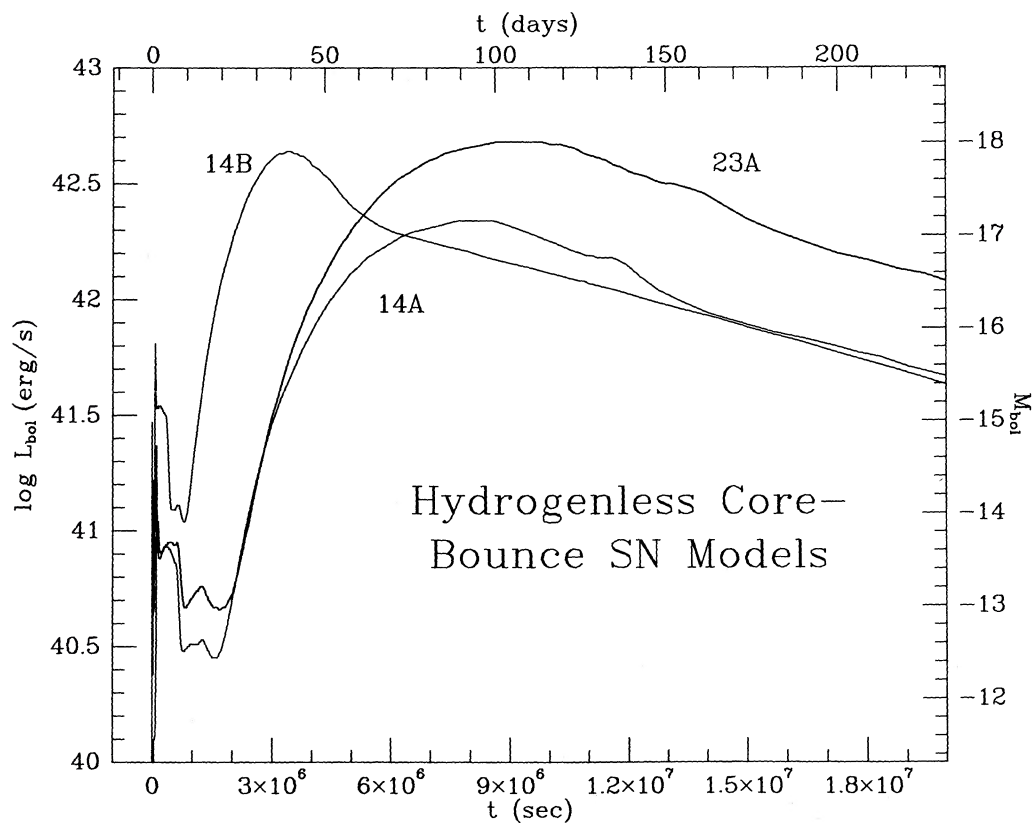


FIG. 2c

TABLE 3  
TIME POINTS FOR MODEL 8A

Point	Time (s)
t1	$4.037 \times 10^4$
t2	$7.678 \times 10^4$
t3	$1.179 \times 10^5$
t4	$1.544 \times 10^5$
t5	$2.013 \times 10^5$
t6	$2.852 \times 10^5$
t7	$4.157 \times 10^5$
t8	$6.177 \times 10^5$
t9	$8.672 \times 10^5$
t10	$1.525 \times 10^6$
t11	$2.769 \times 10^6$
t12	$3.550 \times 10^6$
t13	$4.292 \times 10^6$
t14	$5.101 \times 10^6$
t15	$5.778 \times 10^6$
t16	$7.624 \times 10^6$
t17	$2.802 \times 10^7$
t18	$3.183 \times 10^7$

interior luminosity profile with the location of the  $\tau_e = \frac{2}{3}$  photosphere marked. The photosphere follows the recombination front in, and the luminosity profile flattens behind as the gas becomes optically thin and the radiation is allowed to flow freely. Usually, the photosphere is moving outward in space as matter flows through it. Locations of the photosphere are also indicated on the velocity profile for model 8A in Figure 8. A second recombination front in the trace metals follows the primary, but the drop from  $\log \kappa \sim -2.5$  to  $-3$  (the floor value) has no effect on the light curve. With a non-LTE treatment, the gas would probably not become completely neutral.

Figure 7 also shows the growing accumulation of radioactive decay energy trapped in the optically thick interior. So much energy is released by the decay of  $^{56}\text{Ni}$  (and  $^{56}\text{Co}$ ) that the total internal energy of the ejecta increases by a factor of 6 in spite of expansion losses during the first 17 days after shock breakout. The trapped energy slowly diffuses outward until it meets the recombination front at the base of the helium layer, t9. It is the sudden escape of this energy which sends the supernova light curve to peak. Inspection of Figure 6 reveals that the oxygen layer is reionized slightly by the passage of the decay energy. It is not sufficient to reionize the neutral helium, although it does reionize some of the trace metals once or

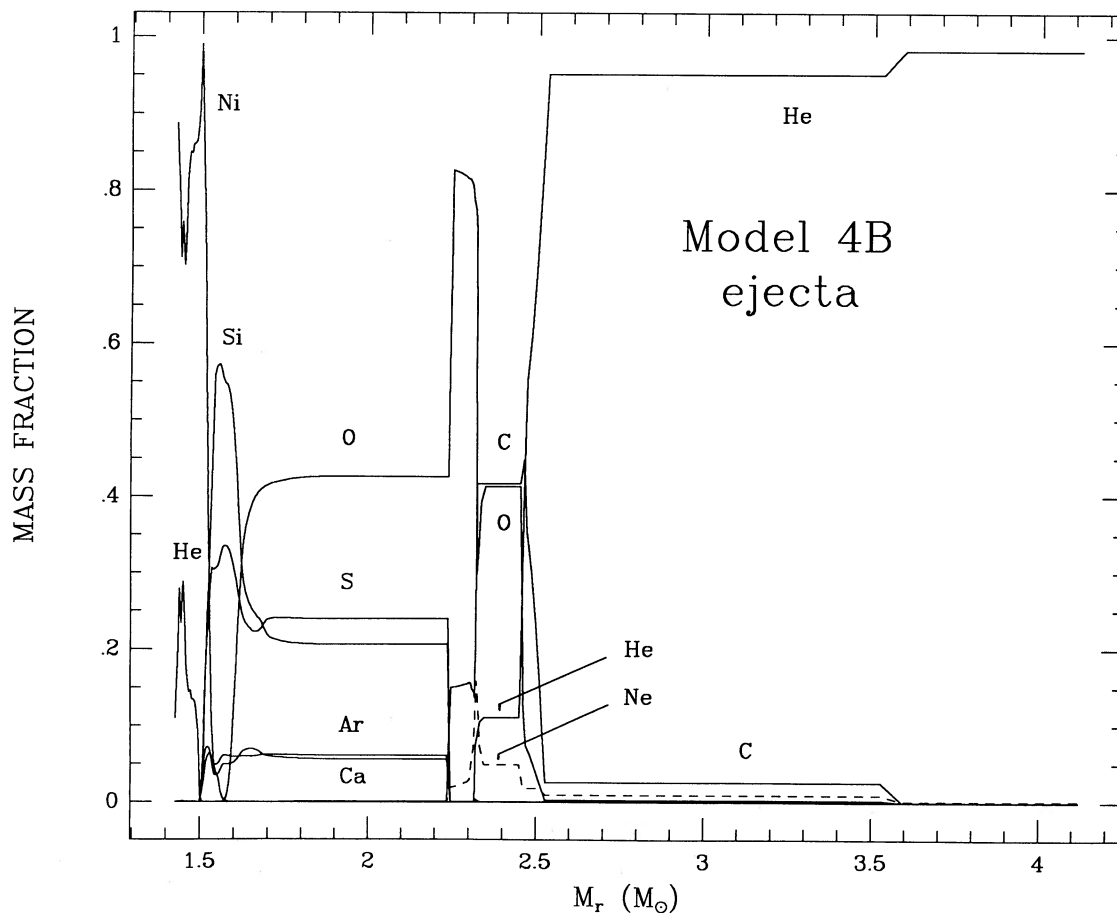


FIG. 3a

FIG. 3.—(a) Composition of the ejecta of model 4B as a function of mass coordinate in the original star. The inner mass zones, not shown, formed the neutron star. The dashed lines are for clarity only. (b) Composition of the ejecta of model 6C as a function of mass coordinate. (c) Composition of the ejecta of model 8A as a function of mass coordinate.

MASS FRACTION

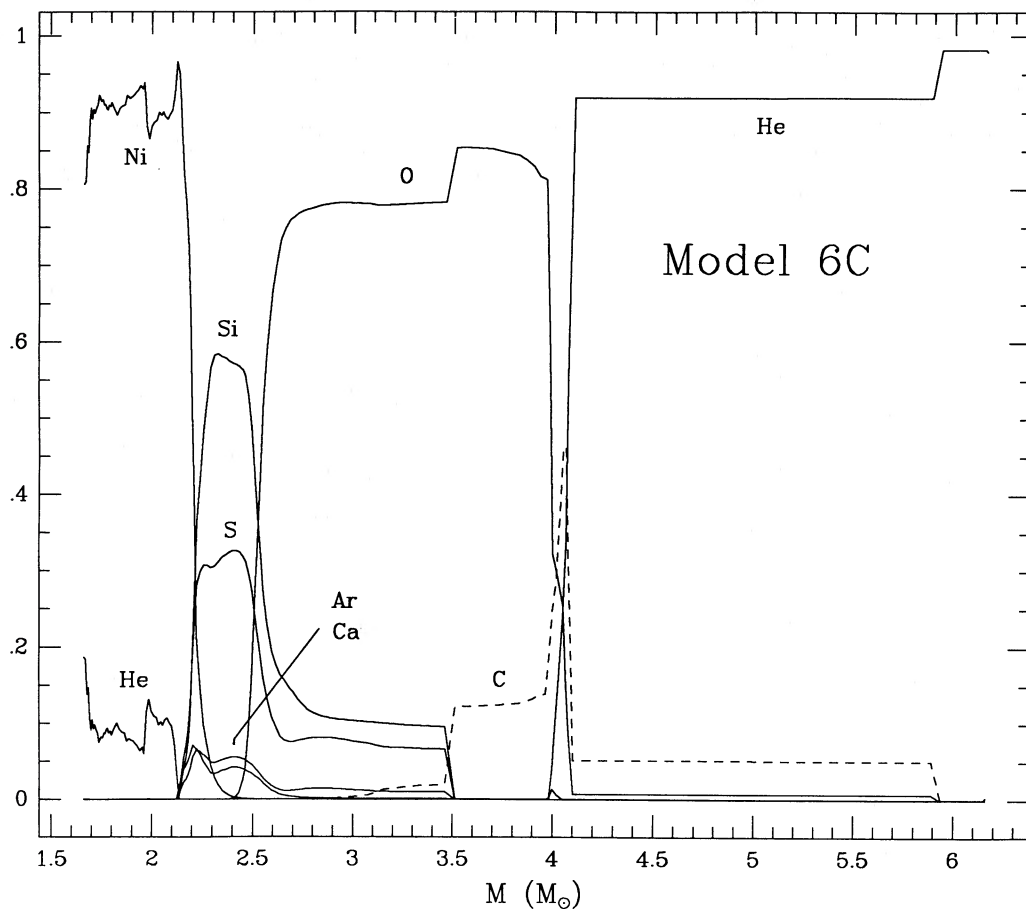


FIG. 3b

MASS FRACTION

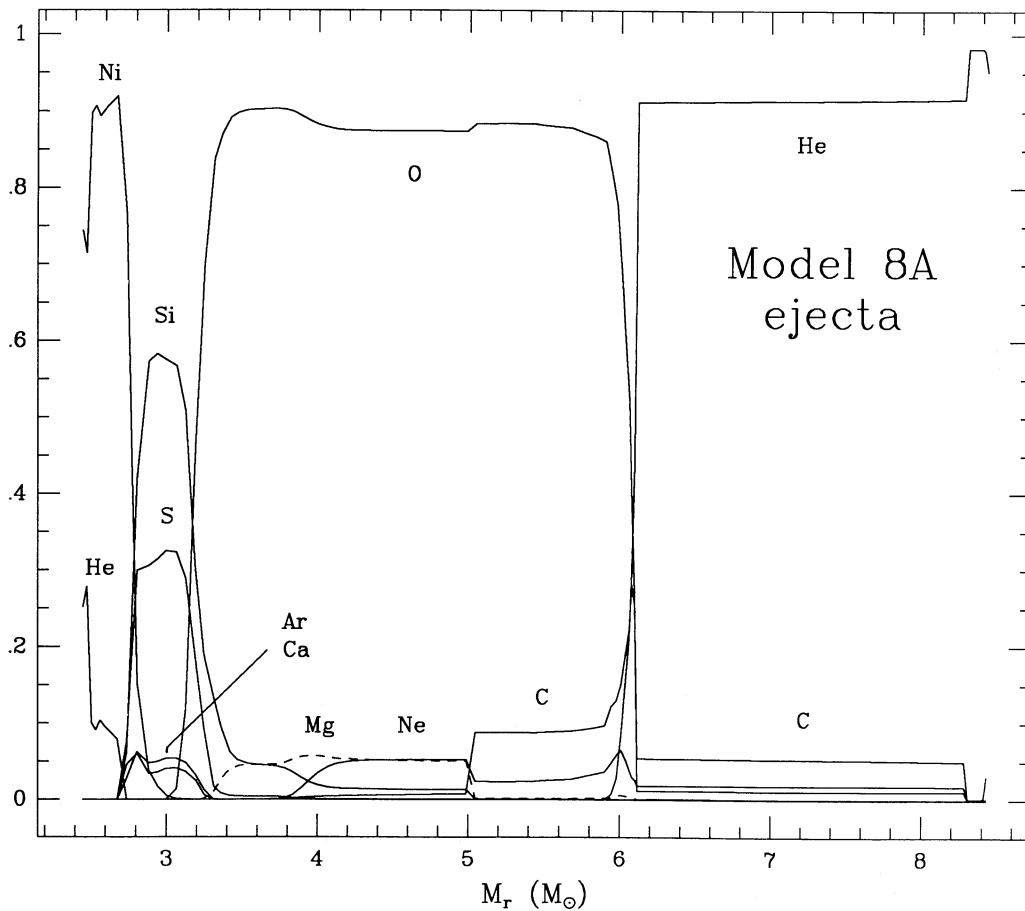


FIG. 3c

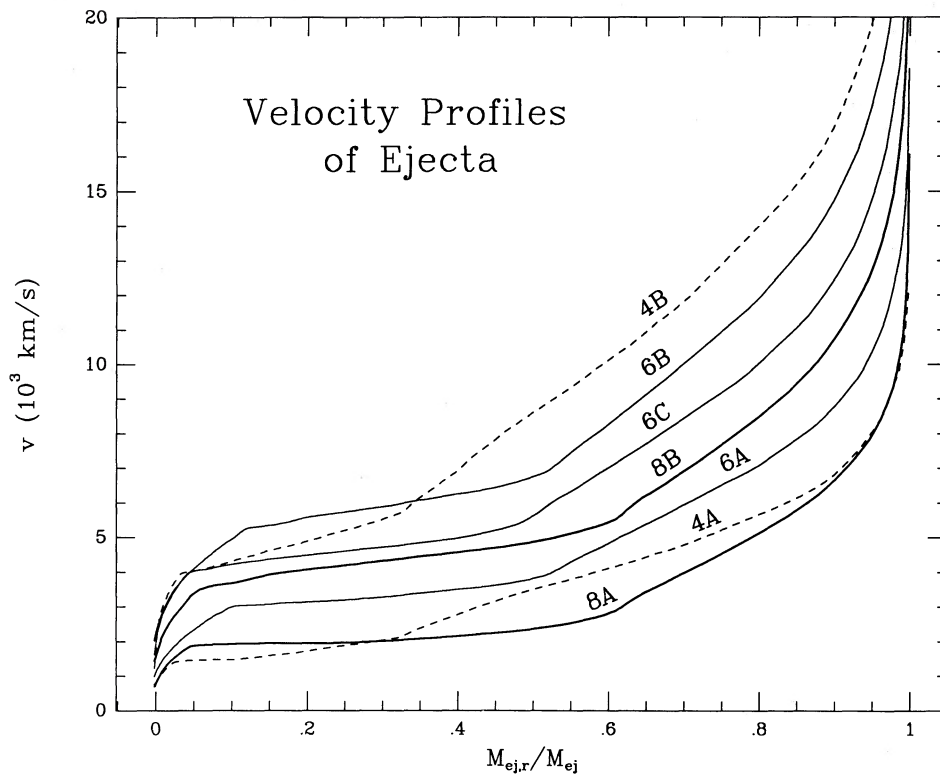


FIG. 4.—Velocity profiles of the ejecta in the 4, 6, and 8  $M_{\odot}$  models as a function of dimensionless mass coordinate. Dashed lines are for clarity only.

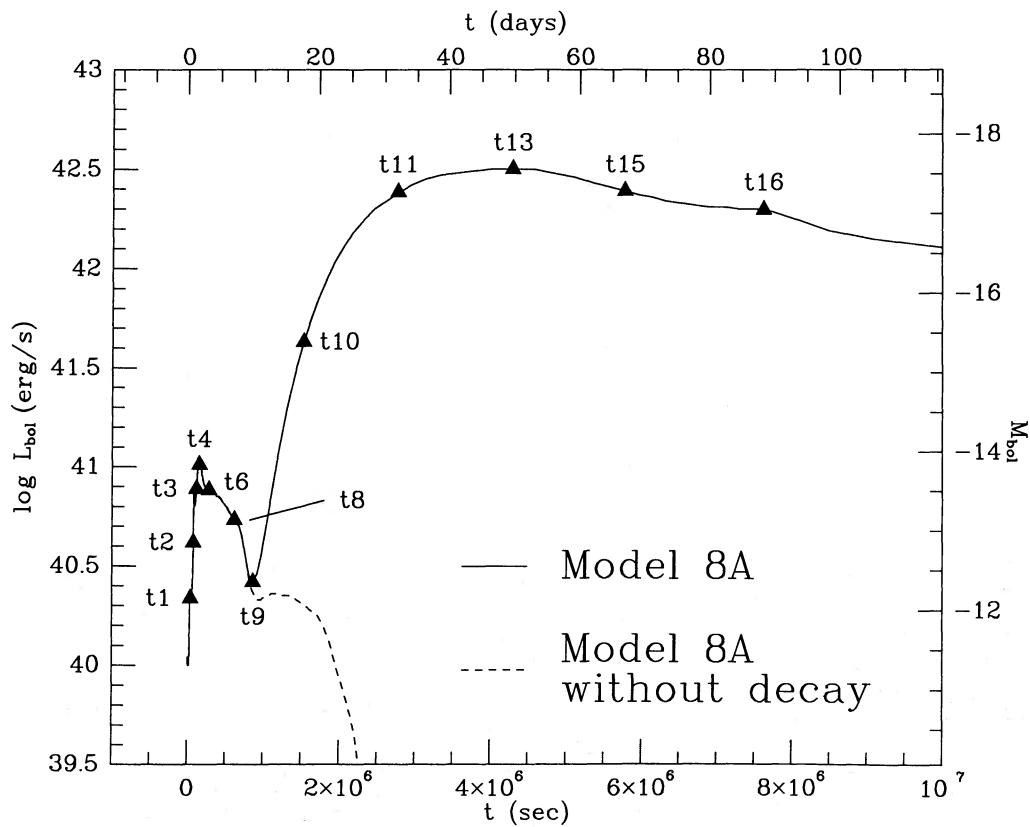


FIG. 5.—Light curve of model 8A with and without deposition of energy from radioactive decay. The labeled points are listed in Table 3 and referred to in the text.

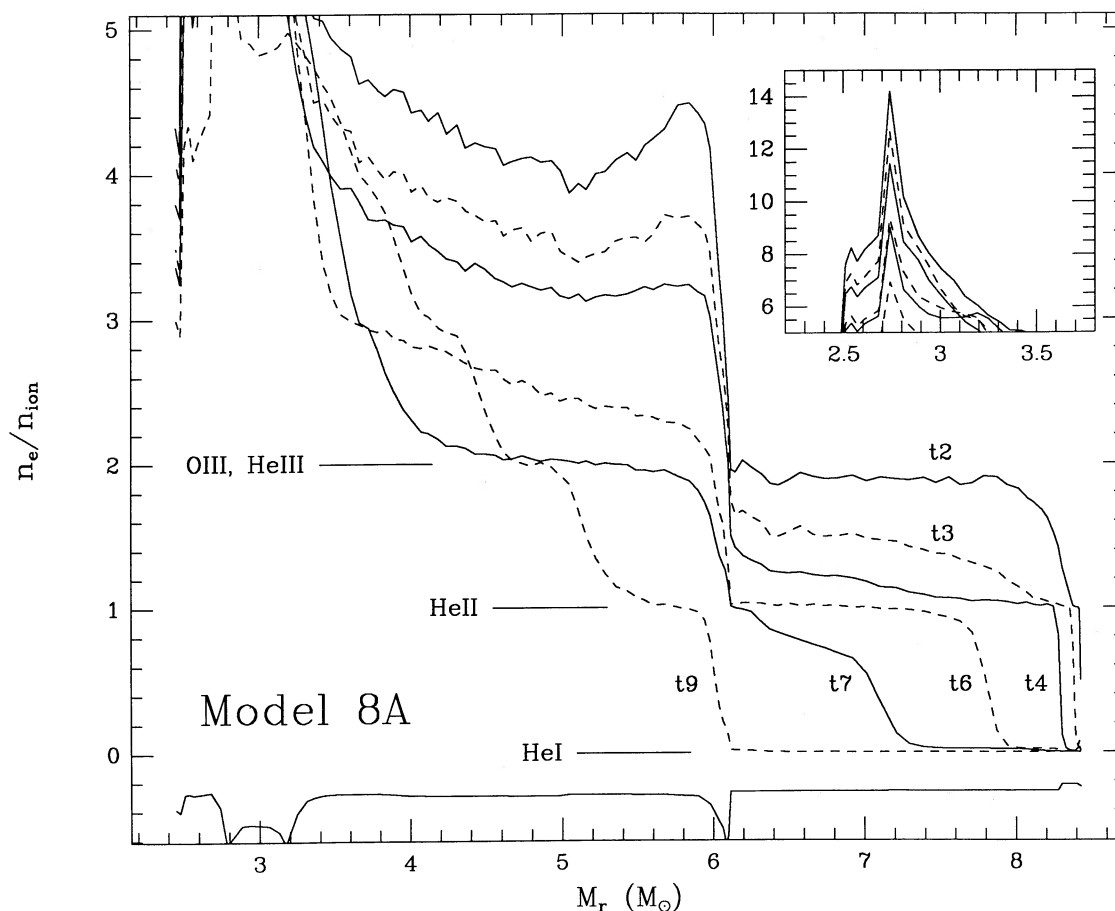


FIG. 6a

FIG. 6.—(a) Recombination occurring during the premaximum display of model 8A. The curves are labeled with times corresponding to points labeled in Fig. 5 and listed in Table 3. The composition is indicated at the bottom (see Fig. 3c). From left to right, there are nickel, silicon, oxygen, and helium layers. Since each layer is predominantly a single element, the electron density divided by the ion density gives the ionization state of the dominant element. Of particular interest here is the recombination of the outer helium layer. Between  $t_2$  and  $t_4$ , the helium goes from being totally to singly ionized. From  $t_4$  to  $t_9$ , the recombination front, defined as the radius outside of which the gas is mostly neutral, can be seen moving through the helium layer. The oxygen layer is also recombining, but the inner portion is reionized slightly at  $t_7$  and  $t_9$  by the diffusing decay energy. (b) Continuation of (a). After  $t_9$ , the helium remains neutral as the oxygen, silicon, and nickel layers progressively recombine. Between  $t_{14}$  and  $t_{16}$ , the recombination front moves through the oxygen layer.

twice. During the rise to peak luminosity, the oxygen layer continues to recombine. Across the rather broad peak between  $t_{11}$  and  $t_{14}$ , an O III to O II recombination wave crosses the oxygen layer, but the true recombination front remains stalled near the outer edge of the oxygen. Between  $t_{14}$  and  $t_{16}$  (the small jog in the light curve), it passes through the oxygen. The silicon and nickel (mostly cobalt by this time) follow over the next 40 days, leaving the whole supernova neutral and optically thin (in our simple prescription) by 128 days ( $t = 1.1 \times 10^7$  s).

The tails of the light curves are also powered by radioactive decay, but the energy deposited is not delayed by having to diffuse through optically thick ejecta. It can escape immediately (i.e., in a time short compared with the expansion time scale, which is equal to the elapsed time for homologous expansion), because the electron scattering optical depth is so low. However, in all cases the ejecta remain thick to gamma rays for an extended period of time. As Figure 9a shows, in model 8A 66% of the decay energy is being absorbed and converted to thermal radiation at 300 days ( $\tau_r$  from the center is 1.7 at 1 MeV). At 600 days the fraction has decreased only to 23%. Figure 9b shows the less massive, more energetic model

6B in which 70% is depositing at 100 days, 10% at 300 days ( $\tau_r = 0.18$ ), and 6% at 600 days. The slope of the tail reflects the radioactive half-life of  $^{56}\text{Co}$  convolved with the decreasing gamma-ray optical depth. A comparison between the gamma-ray deposition derived by KEPLER and that from a more detailed Monte Carlo treatment is discussed in the Appendix. (The tails in Figs. 9a and 9b were computed using the Monte Carlo code.)

Model 8B started with the same presupernova star as model 8A but had a larger explosion energy and produced a narrower, brighter light curve. The same effect can be seen in comparing the  $4 M_\odot$  models, 4A and 4B, and the other pairs of models listed in Table 1. In the 14 and 23  $M_\odot$  models, the trapped decay energy took so long to diffuse out that the recombination front had time to move through about a third (by mass) of the oxygen layer before the two met. The small bumps in the light curves between the helium recombination phase and the main peak are due primarily to the release of radiation trapped in the oxygen.

The brightness and width of Type Ib light curves are determined by the interplay of nickel mass, opacity, and gamma-ray deposition. In general, a greater amount of  $^{56}\text{Ni}$  will brighten

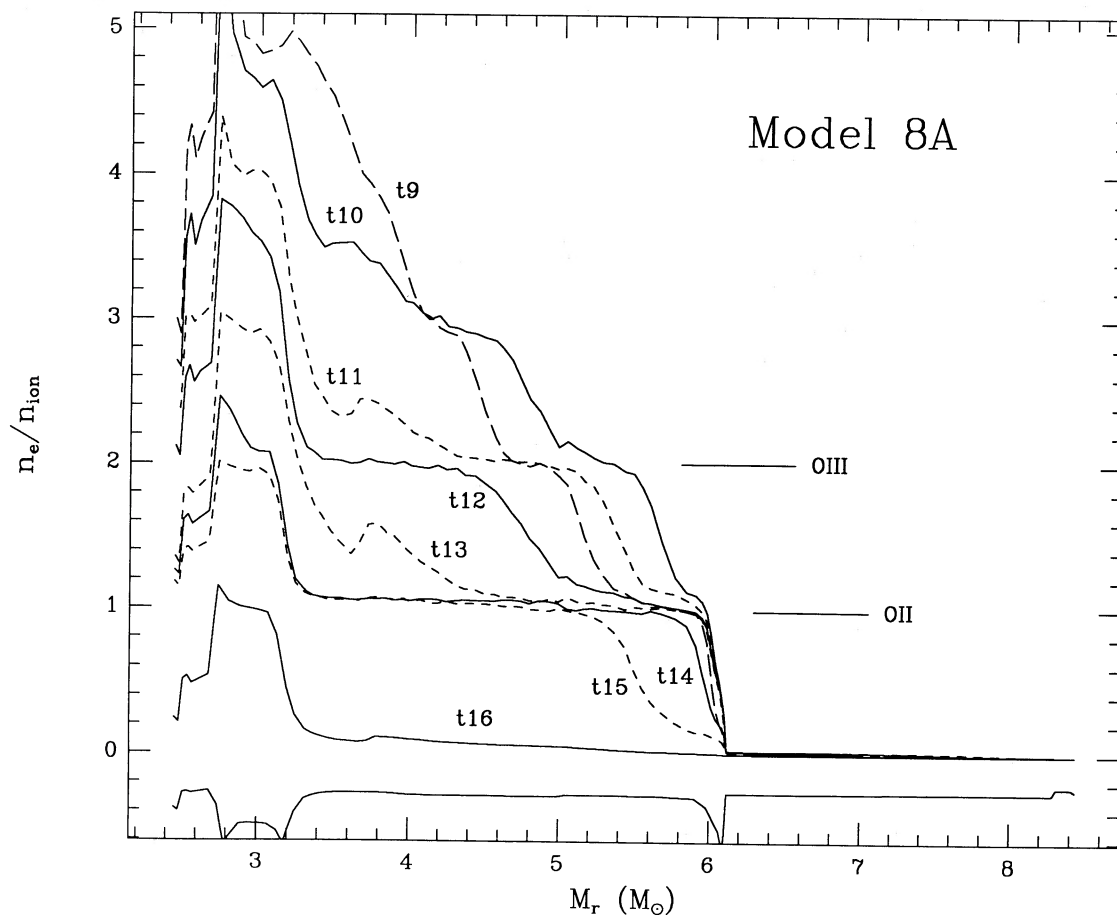


FIG. 6b

and a larger optical depth will broaden a light curve. More nickel is produced by more massive stars which have a shallower density gradient outside the iron core, thus exposing more mass to temperatures conducive to the synthesis of  $^{56}\text{Ni}$ . A stronger explosion will also eject more nickel, as will accreting less mass onto the neutron star during a delayed explosion. The diffusion time is influenced most by the amount of mass the trapped decay energy must diffuse through and the rate at which it thins. Larger stars and lower velocities (weaker explosions) will both give broader light curves.

Note, however, that the relation between nickel mass and peak luminosity is not strictly linear. Some decay energy is used to accelerate the inner layers of the ejecta and produce a "nickel bubble" (see Paper II and Woosley 1988); thus doubling the amount of nickel ejected does not quite double the peak luminosity. Compare, for example, models 6A and 6A-b, 6B-b and so on. For a given amount of nickel, decreasing the total mass will shorten the diffusion time and allow the energy to escape sooner and faster, giving a significantly brighter and narrower peak (compare models 8A and 14A). To a lesser extent, increasing the expansion rate will also shorten the diffusion time (compare 6C and 6B-b). The amount of nickel ejected influences the width of the light curve as well, though not as much as total mass does. Again, compare models in Tables 1 and 2.

The role of recombination energy is subtle and not easily disentangled from the other energy sources available to the supernova. One might expect recombination to be important in SNIb, since their light curves are not dominated by hydro-

gen as are those of SNI. Oxygen, for example, has much higher ionization potentials than hydrogen; but the greatest energy release, which should occur with the first one or two electron captures, happens very early, and the resulting energy is heavily degraded by adiabatic expansion. A "direct" contribution to the luminosity can be made only when the energy is released into an optically thin region, i.e., at or above the photosphere. This can only be the last recombination, which releases relatively little energy. Thus, recombination contributes mainly by keeping the gas hot as it expands. As the most massive models show, the luminosity does not climb much as the recombination wave moves into the oxygen, although the energy released by earlier recombinations has kept the gas hot. Both recombination and thermal energy liberated as the photosphere moves inward in mass are dwarfed by the decay energy once it arrives (the dashed curve in Fig. 5 shows the effect of neglecting decay energy). However, during the pre-maximum display in our models, perhaps half of the luminosity comes from helium recombination. The luminosity during this period is provided only by thermal photons and recombination, and approximately 40%–70% of the internal energy in the layers just inside the recombination front is in the form of ionization energy.

## V. COMPARISON WITH OBSERVATIONS AND DISCUSSION

### a) Widths of Peaks

One must be very careful in comparing models with observed  $B$ - and  $V$ -magnitude light curves because, while the

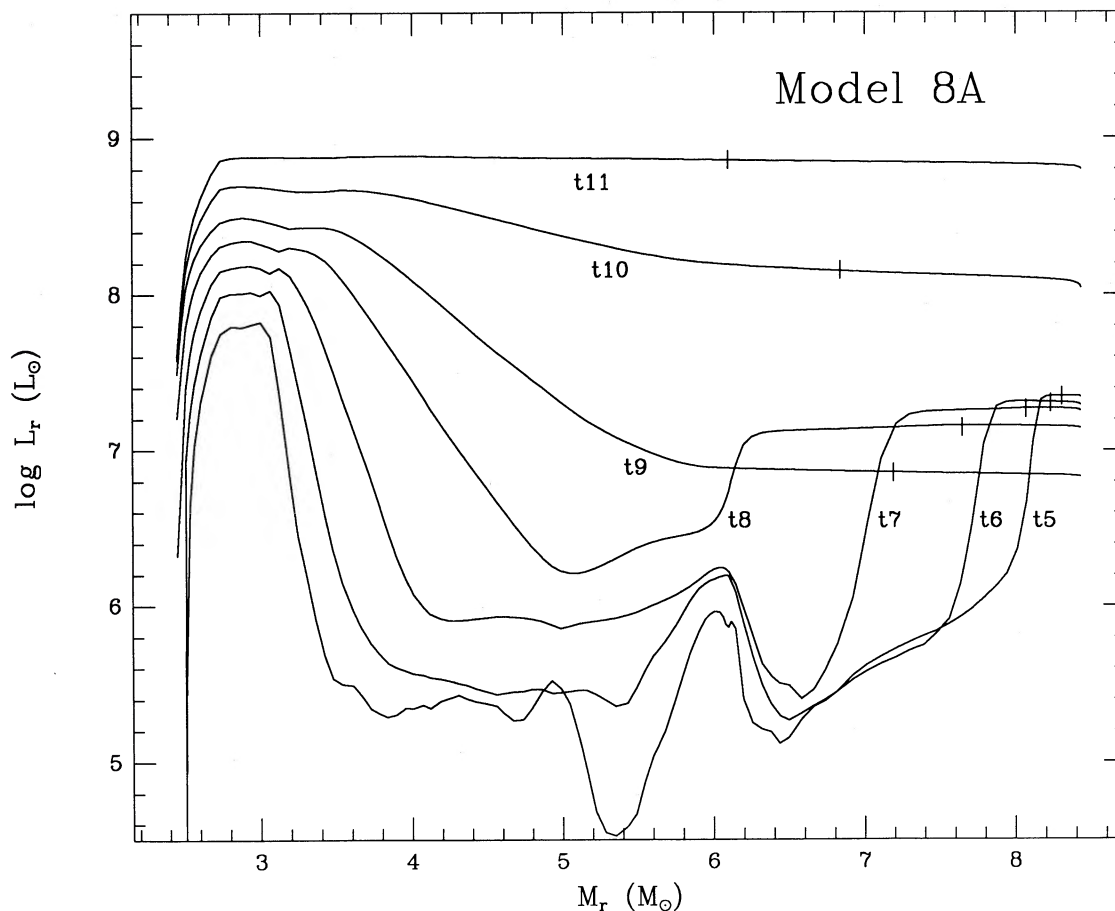


FIG. 7.—Evolution of the interior luminosity profile in model 8A.  $L_r$  is the energy per second flowing through a mass zone. The profile flattens at the surface as the recombination wave moves into the ejecta allowing radiation to travel freely. The photosphere, which is marked by the vertical bars, lags behind the recombination front due to residual optical depth. The accumulation and diffusion of decay energy can be seen in the growing and expanding peak on the left. The wave of decay energy meets the recombination front at  $t_9$ , sending the luminosity to maximum.

calculated bolometric luminosity is fairly well determined, the spectrum is not. It is the spectrum of the emerging radiation which determines the luminosity in each wavelength band. As time passes, the spectrum becomes dominated by emission lines, and a simple blackbody approximation becomes increasingly inaccurate. Further, comparing bolometric luminosity with blue magnitudes is obviously dangerous (cf. Fig. 1*b*). Thus, we prefer to assume that all SNIb have very similar light curves and compare our models with the single bolometric curve presently available, that of SN 1983N. (SN 1985F will be considered separately.)

The bolometric light curve of SN 1983N has a full width at half-maximum luminosity (FWHM, 0.75 mag below peak) of about 25 days (Blair and Panagia 1987). As listed in Tables 1 and 2, our models 4A, 4B, 6B, 6C, 6B-b, and 6C-b have similar FWHM—21–31 days. The more massive models produce light curves which are much too broad to be SNIb. In Figure 10, the 4 and 6  $M_\odot$  models are compared with 1983N directly. The data have been normalized in each case to allow a comparison of shape only. This is justified by the uncertainty in the time and absolute magnitude of peak. (The normalization will be considered separately in § V*d*.) As implied by the widths given in the tables, the fit around maximum light is good for both the 4  $M_\odot$  models and models 6B and 6C. Note that the curves for

models 6A and 6A-b, the least energetic 6  $M_\odot$  models, are definitely too broad. Model 4B provides the best overall fit. It is a bit narrower than SN 1983N, but this is insignificant given the uncertainties in opacities.

The widths of the light curves are fixed mainly by the ejected mass, that is, the time it takes for the trapped decay energy to diffuse through the envelope. Thus, we conclude that not more than about 5  $M_\odot$  of material can be ejected in a typical Type Ib supernova. Allowing for the neutron star remnant, this requires that the progenitors be under 6 or 7  $M_\odot$  at the time they explode. If sources of opacity other than electron scattering are significantly greater than we assumed, even less material can be ejected. One cannot increase the upper limit significantly by simply increasing the explosion energy to shorten the diffusion time. Already, to get a narrow enough curve from a 6  $M_\odot$  star, one needs a very powerful explosion, several times  $10^{51}$  ergs. To get narrow enough curves from the more massive stars, one would have to use explosion energies larger than any calculated SNII explosion model has ever yielded and much greater than that of SN 1987A (Woosley 1988). Model 14B highlights the extreme difficulty of getting narrow peaks from stars over about 10  $M_\odot$ . Even with an explosion energy of nearly  $10^{52}$  ergs (a nontrivial fraction of the total binding energy of a neutron star,  $\sim 3 \times 10^{53}$  ergs,

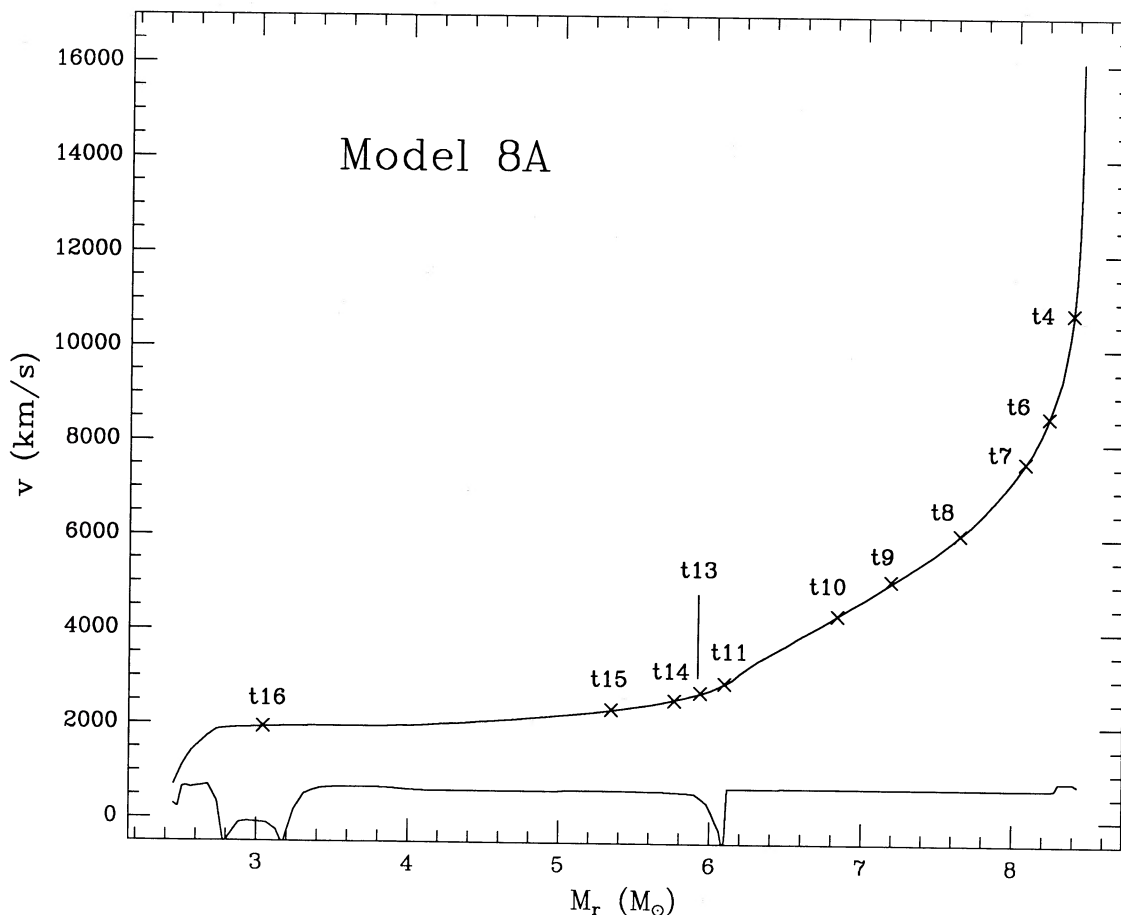


FIG. 8.—Final velocity profile of the ejecta in model 8A. The location of the photosphere is shown at times corresponding to points labeled on Fig. 5 and given in Table 3. Shown along the bottom is an indication of the composition (refer to Fig. 3c).

implying incredibly efficient energy conversion), the FWHM is still 40 days. Constraints provided by the peak luminosity and the slope of the tail also limit the explosion energy.

Although one would expect considerable diversity in the light curves of SNIb if they come from Wolf-Rayet stars, for now we shall continue to treat SN 1985F as a special case. Since it had a broader light curve than the other SNIb in the blue, might it have had a more massive progenitor? The  $B$ -magnitude FWHM of SN 1985F is about 28 days, compared to 21 for the other SNIb. The bolometric FWHM of SN 1983N is about 25 days. If we assume that the bolometric light curve of SN 1985F was also 4 days wider than its blue curve, we get a bolometric FWHM of 32 days for 1985F. This small increase in width cannot support a large increase in progenitor mass. Model 8B is still a week and a half too broad, and model 8A is even wider. Even 6A, the low-energy  $6 M_{\odot}$  model, is several days too wide. To the models which also fit SN 1983N, we can add only 6A-b, the SN 1987A-like model, and model 4B must be eliminated as too narrow. In sum, it is unlikely that the star which produced SN 1985F had a mass over 7 or  $8 M_{\odot}$  at its death, and a  $4-6 M_{\odot}$  progenitor is entirely consistent with the observed light curve.

Our limit of about  $5 M_{\odot}$  of ejecta is in direct contradiction to the conclusions of Begelman and Sarazin (1986), who postulated a  $50 M_{\odot}$  WO Wolf-Rayet progenitor and hence a pair-instability supernova for SN 1985F. Likewise, the spectral analysis by Gaskell *et al.* (1986) found  $\sim 15 M_{\odot}$  of oxygen in

SN 1983N. The limits Begelman and Sarazin derived for the amount of oxygen ejected were actually  $5.6-100 M_{\odot}$ . The lower end of this range is not quite so inconsistent with our limit in terms of *total* mass, but the 4, 6, and  $8 M_{\odot}$  models ejected only 0.4, 1.2, and  $2.6 M_{\odot}$  of oxygen, respectively. On the basis of spectral modeling, Pinto (1988) and Axelrod (1988) have argued that the spectrum of SN 1985F could be produced with as little as half a solar mass of oxygen. In particular, Axelrod (1988) has modeled the late-time spectrum of our model 4B and found that it is in reasonable agreement with the observations.

#### b) Decline from Peak

It is apparent in Figure 10 that, although several of our W-R models can fit the FWHM of SN 1983N, they cannot match the postmaximum decline of the light curve. The models are much too flat. Actually, although the observations are shifted to match the models at peak in Figure 10, they could also be normalized to match on the tail (or the last SN 1983N data point). Observational uncertainties require that the normalization remain arbitrary at this point. But in any case, the models decline less from peak to tail than do the observed SNIb. This lack of contrast is characteristic of the W-R models; all fade only  $\sim 1$  mag between the peak and the start of the tail, regardless of mass. Unless the difference between peak and tail can be increased, or the bolometric light curve of SN 1983N proves not to be representative, the massive star

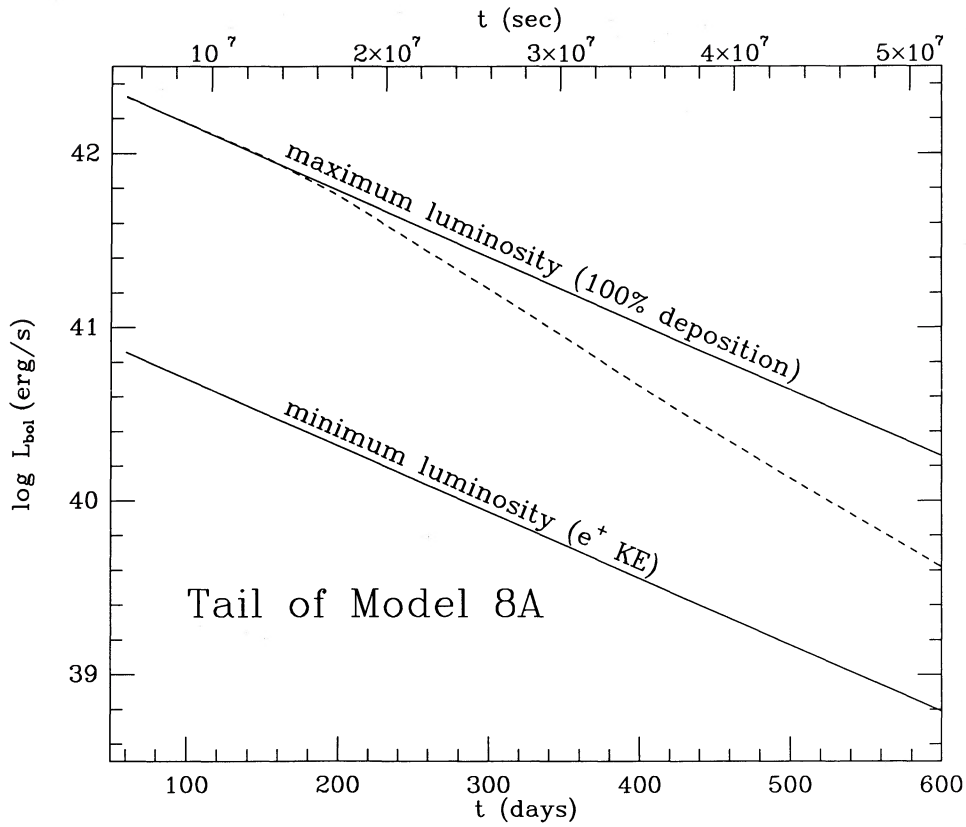


FIG. 9a

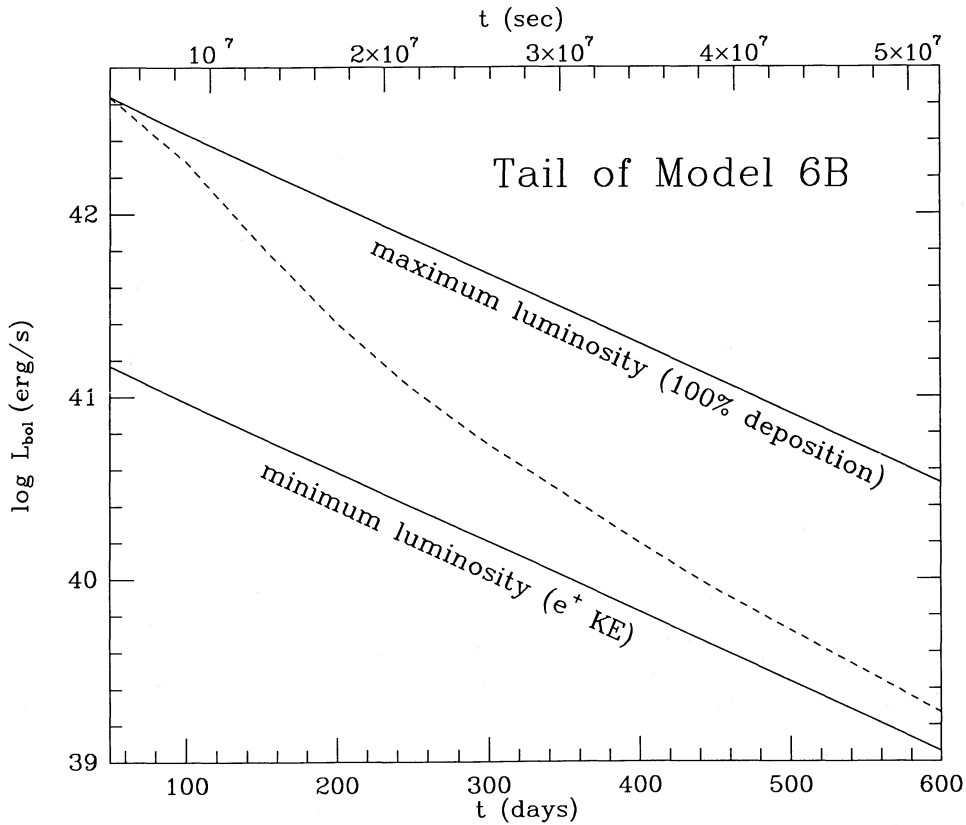


FIG. 9b

FIG. 9—(a) Tail of the light curve of model 8A (dashed line) calculated with the Monte Carlo code described in the Appendix. Also shown are the maximum and minimum amounts of energy that could be radiated. If all the decay energy is deposited and converted to optical radiation which can “immediately” escape, the light curve will follow the upper line. If the ejecta is optically thin to gamma rays, so that no deposition occurs, the light curve will follow the lower line (positron kinetic energy is always assumed to deposit). (b) Same as (a), but for model 6B.

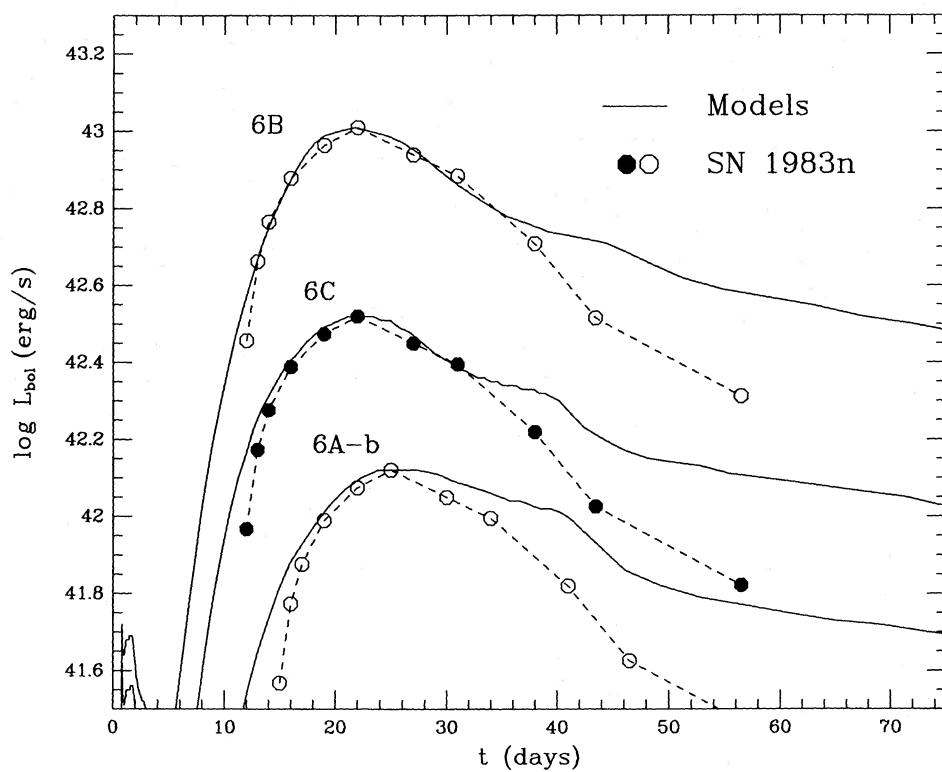


FIG. 10a

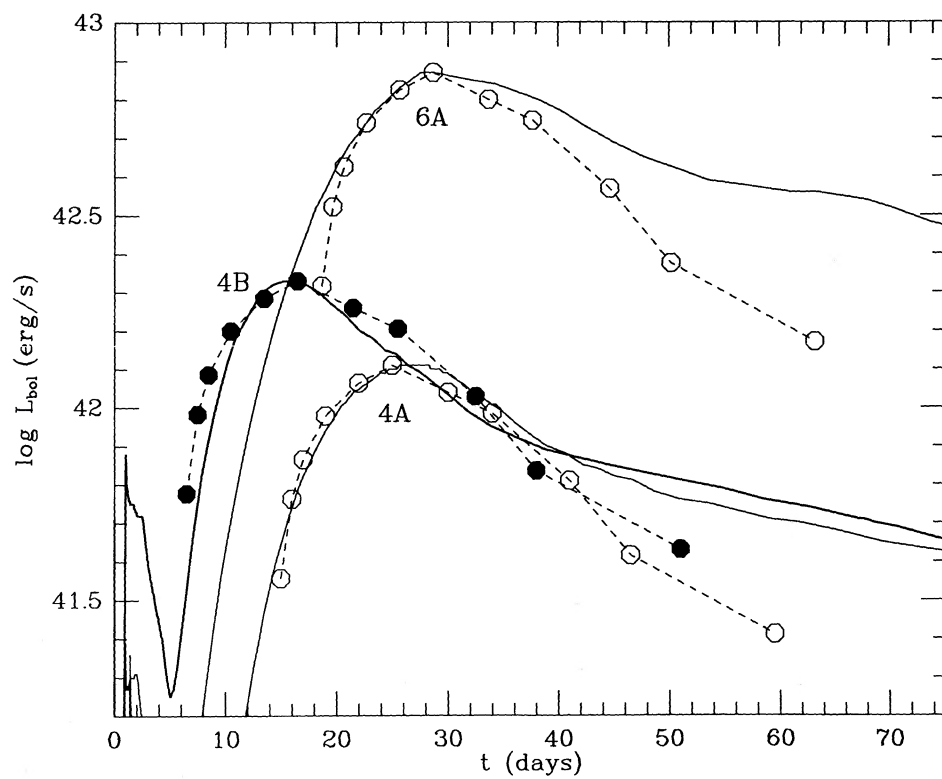


FIG. 10b

FIG. 10.—(a) Bolometric light curve of SN 1983N (Blair and Panagia 1987) superposed on our models 6B, 6C, and 6A-b. Time of peak and maximum luminosity have been arbitrarily adjusted to match the models. (b) Bolometric light curve of SN 1983N superposed on our models 6A, 4A, and 4B.

model for SNIb may have to be abandoned (but see the discussion of SN 1985F).

Many variations on the models in Table 1 were calculated in an attempt to change the peak-to-tail contrast. Increasing the amount of nickel ejected to raise the peak luminosity or decreasing it to lower the luminosity of the tail did not increase the peak-to-tail contrast, since both scale with the amount of nickel ejected. Nor did a modest change in the explosion energy significantly alter the shape of the light curve. Models 6C and 6B-b both ejected  $0.16 M_{\odot}$  of nickel, but model 6C was 1.5 times less energetic. The difference in explosion energy produced only a 2% change in the peak magnitude. It is the amount of nickel which is dominant in determining the peak luminosity; the energy deposited by the shock of the explosion is so heavily degraded that it is insignificant in comparison, and a factor of 1.5 was not enough to affect the diffusion time to a large degree. Neither does mixing of the nickel toward the surface help. A recalculation of model 6A, completely mixed from center to surface, showed that the premaximum display disappears, since the decay energy can begin to escape immediately. This allows the peak to occur a little sooner and broadens it somewhat, but it is not dimmer relative to the tail.

The gamma-ray deposition, which determines the brightness of the tail, was confirmed by the Monte Carlo code (Appendix), but optical opacities are uncertain, particularly when electron scattering no longer dominates. An experiment showed that the optical opacity must be artificially cut by more than half to narrow and brighten the peak significantly. It does not seem reasonable to suppose that the opacity could be so far below the LTE electron scattering value; rather, the opacity would

probably be higher because of lines and bound-free edges. If non-LTE effects or lines gave an opacity much larger than  $10^{-3} \text{ cm}^2 \text{ g}^{-1}$ , less of the reprocessed decay energy could escape, lowering the luminosity early on the tail. However, the widths of the light curves would also be increased substantially, and the luminosity at peak would be lowered as well. As described in § Vd. the models are already on the dim side. To narrow and brighten the light curves again, one would need to invoke very powerful explosions. A smaller progenitor would also have a narrower curve, but below  $\sim 4 M_{\odot}$  very little  $^{56}\text{Ni}$  is produced and the supernova would be too dim.

One way, perhaps the only way, to render the massive-star model for SNIb consistent with the current data is to decrease the efficiency of gamma-ray deposition early on the tail (as occurs naturally in the case of SNIa). A possible mechanism is clumping of the ejecta. If, at the start of the tail, all the matter has coalesced into clouds (to take an extreme case), more of the gamma rays from decay will be able to escape, lowering the "bolometric" luminosity. Comparing model 6B (Figs. 10a and 9b) with SN 1983N, one can see that to match the last observed point, the deposition fraction would have to drop from the current 100% to about 70%. As an experiment, to simulate the effect of clumping, we reran model 6B several times with smaller gamma-ray opacities. This had the effect of changing the average gamma-ray optical depth ( $\tau_{\gamma} = \kappa_{\gamma} \int \rho dr$ ). The results are shown in Figure 11. With  $\kappa_{\gamma} = 0.003 \text{ cm}^2 \text{ g}^{-1}$  we can match the observations of SN 1983N quite well. This model also matches the observations of the SNIa 1972E, because it simulates the effect of lowering the mass and increasing the expansion velocity. Whether the extreme density inho-

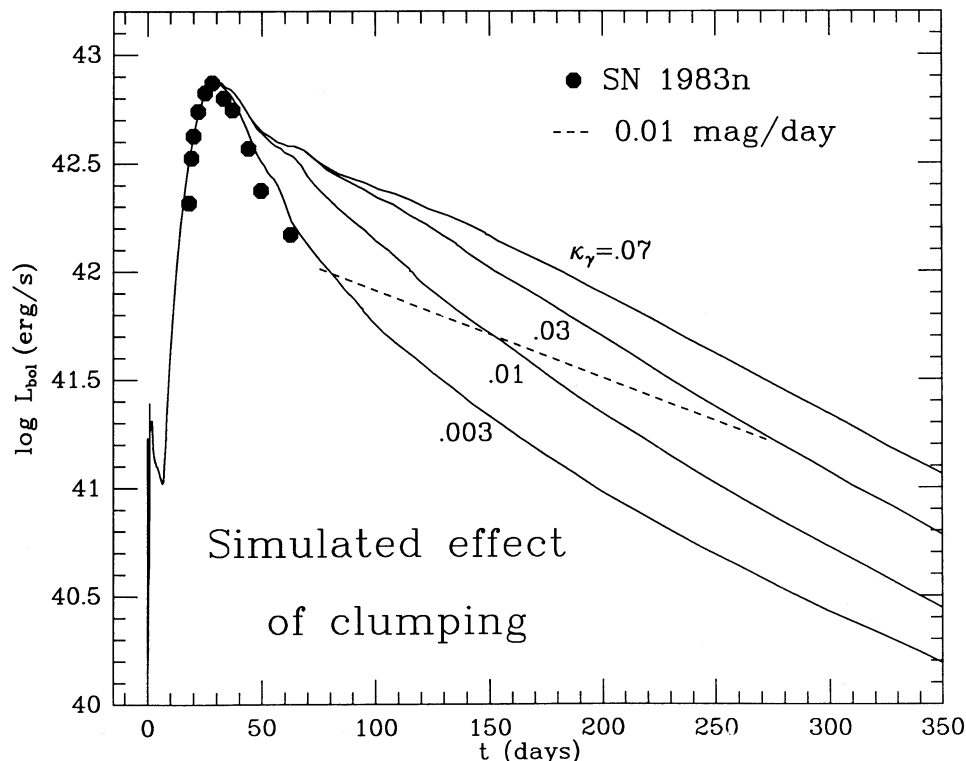


FIG. 11.—Light curve of model 6B assuming various values for the effective gamma-ray opacity. The normalized data for SN 1983N are superposed, showing that a very small  $\kappa_{\gamma}$  must be used to match the observations;  $\kappa_{\gamma}$  always occurs multiplied by the column depth in the calculations, so the use of a smaller opacity may also simulate a decrease in the average column depth. Clumping of the ejecta may provide a mechanism for doing so. The dashed line shows, for comparison, the slope obtained from 100% deposition of  $^{56}\text{Co}$  decay energy.

mogeneities required to explain the observations really exist requires further study. For now, it remains an interesting but arbitrary exercise.

While the (unmodified spherically symmetric) models are too flat to match the light curve of SN 1983N, they may fit SN 1985F. Comparing the blue light curves of SNIb, it is evident that SN 1985F declines less after peak than does 1964L; SN 1962L may lie between the two. The significance of the differences, particularly for SN 1962L, is not clear. Obviously, careful subtraction of the underlying galaxy is important at late times, and we have no information with which to make an assessment of the accuracy of the data. The SNIb apparently decline more slowly and by a lesser amount in the bolometric than in the blue (Fig. 1). The same is true for SN 1987A (Catchpole *et al.* 1987). Schurmann (1983) found the effect theoretically when he used a truncated blackbody spectrum to convert bolometric magnitudes to blue magnitudes for SNIa models. We can say that if SN 1983N had the same blue light curve as SN 1964L, and the difference between the bolometric and *B*-magnitude light curves was the same for SN 1985F, then the bolometric light curve of SN 1985 would have dropped only  $\sim 0.8$ – $1.0$  mag after peak. Thus, it is possible that the progenitor of SN 1985F was a W-R star.

#### c) Slope of the Tail

Observations of the slope and overall brightness of the exponential tail of a Type Ib supernova (bolometric) would provide information important in determining the explosion energy, the amount of mass ejected, the abundance of  $^{56}\text{Ni}$ , and possibly the extent of clumping. It is very unfortunate that the observations of SN 1983 ended at such a critical time. The only late-time data that we have are *B*-magnitudes for SN 1964L and SN 1985F (Fig. 1c). Intriguingly, the *B*-magnitude tails have approximately the same decay rate as  $^{56}\text{Co}$ . If it were the case that the bolometric traced the blue, some very interesting conclusions could be drawn about SNIb (these will be described below). However, it is not at all clear whether this assumption is correct.

On the other hand, as seen in Figures 1a and 1b, the bolometric light curve follows the visual very well, at least as far as the data extend, but not the blue. If this trend continues, the bolometric tail will not have the same slope as that in the blue, unless the two later become parallel. Further, one might expect that given the close similarity of SNIa and SNIb in *B*- and *V*-magnitudes, SNIa and SNIb would be very similar in bolometric magnitude also; and, indeed, this contention is borne out for the data in hand. The SN 1983N data points lie along the bolometric light curve defined to about 80 days past peak by the SNIa 1981B and 1972E (Graham 1986b; Axelrod 1980). The bolometric data from both these supernovae follow the mean *V*-magnitude light curve of SNIa. (The *B* and *V* data for SN 1981B [Barbon, Ciatti, and Rosino 1982] lie along the corresponding mean Type Ia light curves, showing that they are not peculiar in any way.) On the other hand, one must remember that as the spectra evolve, different spectral lines become dominant in SNIa and SNIb, and there is no reason to expect that their blue, visual, and bolometric light curves should continue their early similarity. In fact, at late times, SNIb do not fade as fast as SNIa in the blue (Fig. 1c). The particular slope of the SNIb *B*-magnitude tails, 0.01 day, makes it tempting, and not unreasonable, to suppose that the bolometric luminosity becomes parallel to the blue on the exponential tail at about 40 days past maximum.

If the bolometric luminosity traced the blue, the decay rate of 0.01 mag per day for over 300 days would imply that a constant fraction (presumably 100%) of the decay energy was being absorbed by the ejecta for an extended period of time. To fade so gradually, a model must be massive and/or expand relatively slowly. Some of the W-R models can match this rate of decline, but many fade at a faster rate. Because of the small amount of mass and the large velocities involved, the deposition fraction in Type Ia supernovae, and, by implication, in white dwarf models for SNIb, does not remain constant for so long, hence they have steeper tails.

While awaiting future observations that will decide the question, the composite data set can be used with various assumptions to estimate the amount of  $^{56}\text{Ni}$  ejected by Type Ib supernovae. We assume that (1) the bolometric light curve of SN 1983N and the blue light curve of SN 1964L are representative of SNIb, (2) the bolometric tail is  $\sim 0.8$  mag brighter than the blue (cf. Fig. 1) at least at the beginning (near the last SN 1983N data point), and (3) 100% of the decay energy is being reemitted as thermal radiation at that time. The "observed" bolometric magnitudes at peak (Fig. 12, § Vd) then imply that Type Ib supernovae eject  $\sim 0.1$ – $0.4(H_0/50)^{-2} M_\odot$  of  $^{56}\text{Ni}$ . For only 70% deposition (see § Vb), we obtain  $\sim 0.1$ – $0.6(H_0/50)^{-2} M_\odot$ . In either case, the nickel mass is consistent with that inferred for SN 1983N by Graham *et al.* (1986), within the uncertainties, and comparable, at the lower end, to that from SN 1987A (Woosley 1988) and SN 1980K (Uomoto and Kirshner 1986). The variation in peak luminosity and hence nickel mass from event to event may or may not be intrinsic.

#### d) Peak Magnitudes

It has often been claimed that Type Ib supernovae are 1.5–2 mag fainter than Type Ia supernovae at peak, but is this true, and with what qualifications? There is considerable disagreement in the literature about the distances to the observed SNIb, and the extinctions produced by our own and the host galaxies are uncertain. To get a consistent sample of actual Type Ib peak luminosities to compare with SNIa and our models, we have recomputed the absolute magnitudes of SN 1962L, 1964L, 1983N, 1984L, and 1985F using peak apparent magnitudes from Bertola (1964), Bertola, Mammano, and Perinotto (1965), Sramek, Panagia, and Weiler (1984), Wheeler and Levreault (1985), and Tsvetkov (1986); galactic velocities and coordinates from the *Revised Shapley-Ames Catalog of Bright Galaxies* (Sandage and Tammann 1981); a Virgocentric infall model from Aaronson *et al.* (1982, solution [3.1]), and Galactic extinctions as given by Burstein and Heiles (1984). To estimate magnitudes of the Type Ib's in the unobserved or unpublished spectral ranges, we have used published colors near maximum or assumed  $B-V = 0.45$ – $0.6$ , typical values for SNIb (Harkness *et al.* 1987 and references therein). We also used  $B = m_{\text{pg}} + 0.3$  if needed. The results are given in Figure 12 for  $H_0 = 50$ . The lengths of the lines roughly indicate the uncertainties in apparent magnitudes and distances (the latter taken only from errors in velocities given in the Shapley-Ames catalog). Unfortunately, only SN 1983N has been observed over a wide enough frequency range to derive a bolometric magnitude (by direct integration of spectra; Blair and Panagia 1987). Values for the other SNIb will lie within the box if their bolometric corrections are the same as that of SN 1983N.

The comparison between observed SNIa and SNIb is also hampered by the lack of any precise observationally deter-

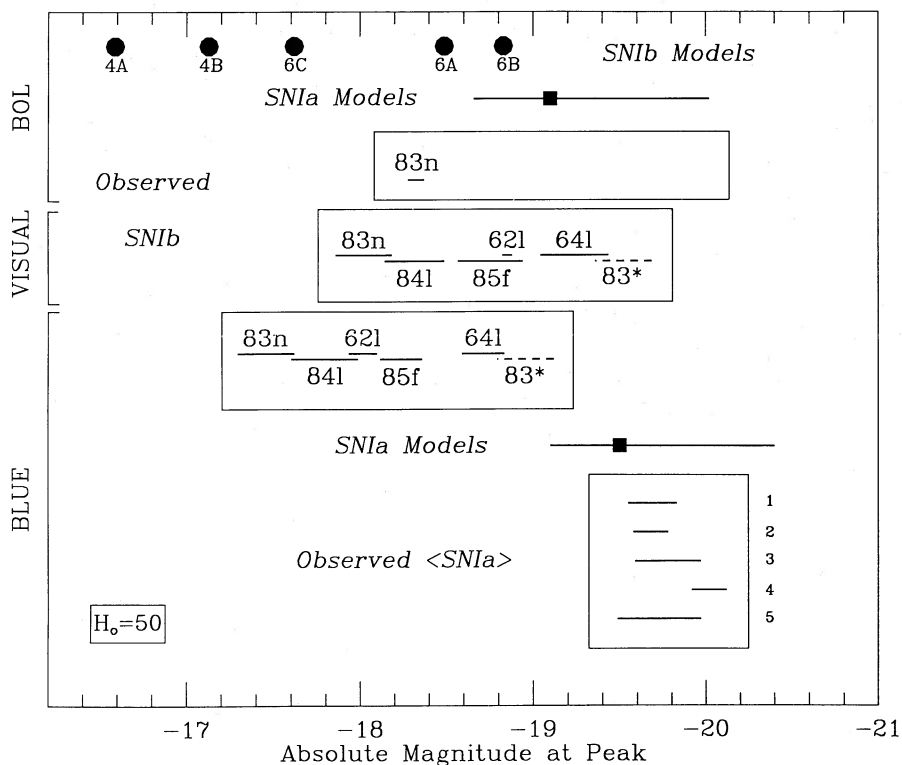


FIG. 12.—Comparison of peak magnitudes. Shown are bolometric,  $V$ , and  $B$  peak magnitudes of various objects. At top are our Type Ib models. The boxes in the center encompass observed and estimated values for actual Type Ib supernovae (see text). The label 62l refers to SN 1962L, etc., and 83\* refers to SN 1983N, including 1.5 mag of intrinsic absorption. The bars labeled *SNIa models* extend from the peak luminosity implied by the production of  $1.4 M_{\odot}$  of  $^{56}\text{Ni}$  to that implied by  $0.4 M_{\odot}$ . The favored value of  $0.6 M_{\odot}$  of  $^{56}\text{Ni}$  is indicated by the solid square. The corresponding blue magnitudes were calculated assuming a blackbody spectrum truncated at  $4000 \text{ \AA}$  (Arnett, Branch, and Wheeler 1985). The lower box encloses various determinations of the mean Type Ia peak  $B$ -magnitude with error bars. In key at right of box, 1 = Tammann (1982); 2 = Branch and Bettis (1978), the whole sample; 3 = Branch and Bettis (1978), only those in ellipticals; 4 = Branch and Bettis (1978), those with velocities greater than  $1500 \text{ km s}^{-1}$ ; 5 = Sandage and Tammann (1982).

mined absolute magnitudes for Type Ia supernovae. Values for  $\langle M_B \rangle$  given by a number of authors are shown in Figure 12. The lengths of the lines show the uncertainty in the mean value; the dispersion of individual SNIa about the mean is presumably only about 0.25 mag to either side (Doggett and Branch 1985). Also shown in Figure 12 are the allowed range and preferred value from white dwarf deflagration models (Arnett, Branch, and Wheeler 1985). The blue magnitudes were calculated assuming a blackbody spectrum with the emission truncated shortward of  $4000 \text{ \AA}$ . The fact that the absolute blue magnitude is smaller than the bolometric magnitude is not necessarily surprising, since the magnitude scales are independent of each other, i.e., they have different zero points.

As is apparent from Figure 12, in the blue, the *mean* SN Ib is indeed about 1.5 mag fainter than the average SNIa (and comparable to Type II supernovae at peak), but not *all* Type Ib's are necessarily 1.5 mag dimmer than all Type Ia's. Branch's (1986) analysis also showed that some SN Ib are as bright as some SNIa. If SN Ib do have Wolf-Rayet-like progenitors, one would expect a range of peak luminosities to exist as a result of varying core masses, explosion energies, and amounts of mass loss. Differences might also arise from variations in the amount of  $^{56}\text{Ni}$  ejected. It is not known, from either observations or theory, whether all cores of the same mass will eject the same amount of nickel. On the other hand, the large magnitude range covered by the Type Ib's could be caused, partially or wholly, by uncertainties in distances and extinctions. Since they occur in spiral arms and H II regions and may have sub-

stantial circumstellar shells, they would be expected to have large and varying amounts of intrinsic extinction which have not been accounted for. Balmer line ratios for 30 H II regions in M83 indicate a spread in  $A_V$  of 0.1–3 (see references in Graham *et al.* 1986), and Graham *et al.* (1986) estimated about 1.5 mag of extinction in the vicinity of SN 1983N. In Figure 12, "83\*" shows the effect of including this absorption ( $A_V = A_B = 1.5$  assumed). *If the other SN Ib have as much intrinsic absorption, the mean Type Ib could be as bright as the mean Type Ia!*

It is interesting that the 1.5 mag difference seen in  $B$ -magnitude does not extend to  $M_{\text{bol}}$ . The same effect can be seen when comparing SN 1987A with normal SNIa in the blue versus the bolometric. Although we do not have an average observationally determined bolometric magnitude for SNIa at peak, we believe that the models are fairly reliable, particularly the bolometric luminosities. For comparison, the absolute bolometric magnitude of the SNIa 1972E (Graham 1986b), using a distance calculated as for the SN Ib, lies within the theoretical limits ( $M_{\text{bol}} = -19.5$  to  $-19.6$ ). The smaller difference between SNIa and SN Ib in the bolometric may be at least partially explained by the fact that SN Ib are redder than SNIa. The exact form of the spectrum is crucial, and comparisons in various bands can give different results.

Of the models, the brightest, 6A and 6B, reach peaks comparable to the "observed" peak bolometric magnitudes. The others are too dim. However, absolute magnitudes based on observed apparent magnitudes (those in boxes in Fig. 12) depend on the assumed value of  $H_0$ . If  $H_0 = 100$ , distances are

halved and the objects shift 1.5 mag to the left in the figure. Models 6C and 4B then become more acceptable. Stars having helium cores lighter than  $4 M_{\odot}$  would eject less nickel than model 4A (Mayle and Wilson 1988) and be even fainter, much too faint to be SNIb.

As noted in § Vb, the difference between the luminosity at peak and the luminosity at the start of the tail is smaller in the models than was observed in SN 1983N. Hence, a comparison of tail luminosities will yield different results than the comparison of peak magnitudes. In fact, for  $H_0 = 50$ , all the 4 and 6  $M_{\odot}$  models are bright enough after the initial drop from peak to match SN 1983N at the corresponding time. If  $H_0$  is larger, the more energetic 6  $M_{\odot}$  models become too bright. This implies that, if there is 100% deposition of decay energy in SNIb at the start of the tail, the models contain approximately the correct amount of  $^{56}\text{Ni}$  and for some reason, the "light-to-nickel ratio" is not large enough at peak.

e) *Original Mass of a Type Ib Progenitor and the Relation to Wolf-Rayet Stars*

Overall, the model that best fits the observations of SN 1983N is model 6C, with 4B a close second. The major objections to each model are listed in Tables 1 and 2. Model 4B had the best overall shape, but its explosion energy was high and its peak luminosity was rather low. (However, the explosion energy can be changed by perhaps a factor of 2 without affecting the light curve very much.) Model 6C was acceptable on all points except that which all the models failed: the contrast between peak and tail.

Several things have been deduced thus far about the characteristics of SNIb progenitors, assuming of course, that they are massive stars. First, since they show helium at early times, but no hydrogen or oxygen, they must have lost their hydrogen envelopes but retained at least some of the underlying helium layer. Second, the width and luminosity of the light curve constrain the total mass of the star to lie between about 4 and 7  $M_{\odot}$ .

Considering the composition profiles in Figure 3 and the surface composition plots in Maeder (1987), one is then led to the conclusion that the SNIb seen so far could come only from stars having main-sequence masses in the 15–25  $M_{\odot}$  range. A 25  $M_{\odot}$  main-sequence star could become a Type Ib progenitor if it lost all its hydrogen and nearly all its helium to become, at death, a 7  $M_{\odot}$  W-R star. If it did not lose that much helium, it would be too massive to match the observed light curve width. Stars heavier than 25  $M_{\odot}$  are effectively ruled out by the fact that they would be too massive even if they were stripped down to the oxygen layer. On the other hand, to avoid too narrow a light curve, a 15  $M_{\odot}$  main-sequence star could lose practically no helium (thus it would be a W-R star for only a very short time). Including more opacity might broaden the light curves enough to allow some helium to be lost from the 15  $M_{\odot}$  star. A smaller star would have a helium core under 4  $M_{\odot}$ , so too little mass would remain even if it lost only its hydrogen, and such stars would produce much too little  $^{56}\text{Ni}$  and be too dim regardless of the amount of mass loss. Between 15 and 25  $M_{\odot}$ , various amounts of helium loss could occur, giving the range of helium masses postulated by Wheeler *et al.* (1986). For example, a 20  $M_{\odot}$  star would go from 6 to 4  $M_{\odot}$  as it lost its helium. These figures could be modified slightly if mass-loss rates were high enough to affect the formation of the helium or carbon-oxygen cores by cooling material that would have burned in the absence of mass loss. There are also uncertainties

in the association between model helium core mass and main-sequence mass due to variations in the convective algorithms (e.g., convective overshoot; see Maeder and Meynet 1987) and nuclear reaction rates used by various researchers.

One must now ask whether such stars actually exist and, in particular, whether they could be Wolf-Rayet stars, as has been suggested. There are three basic types of W-R stars: WN, WC, and WO. Hydrogen has been detected in some WN stars, but Wolf-Rayet stars are notable for the absence of this element (Chiosi and Maeder 1986). Presumably, a star progresses through the sequence as mass loss uncovers deeper and deeper layers of the star, exposing first the products of hydrogen (CNO) burning, then of helium burning (Maeder 1987; Chiosi and Maeder 1986). At least one-third of Wolf-Rayet stars are found in binary systems. Their masses range from about 10 to 50  $M_{\odot}$  with a mean of 20  $M_{\odot}$ , and there is no simple relation between mass and type (Massey 1982; Conti 1986).

The large masses of observed W-R stars present a problem for the hypothesis that SNIb originate in Wolf-Rayet stars, because the light curves of supernovae in 10–50  $M_{\odot}$  stars would be too broad (Tables 1 and 2). A 10  $M_{\odot}$  W-R star might be able to lose a few more solar masses by the time of the explosion, but the restriction that mass loss can proceed only to the bottom of the helium layer means that only a small fraction of those now 10  $M_{\odot}$  will produce SNIb. It is somewhat simpler to compare the main-sequence masses of the current W-R stars to the range allowed for SNIb. Many estimates have been made for the former, based on observed characteristics of the W-R population, cluster membership, and theory, with results ranging from 20 to 40  $M_{\odot}$  (Schild 1986; Maeder 1984; Conti 1984; Abbott *et al.* 1986). Composition and surface abundance plots (Fig. 3; Maeder 1987) imply that the minimum initial mass of existing W-R stars is about 25  $M_{\odot}$ . Again, we are led to the conclusion that very few W-R stars will end as SNIb.

The mass loss which produces Wolf-Rayet stars usually proceeds via a strong stellar wind (Abbott *et al.* 1986). Evolutionary models including mass loss and binary star evolution (Chiosi and Maeder 1986; Maeder and Meynet 1987; de Loore 1986) indicate that *single* Wolf-Rayet stars originate from main-sequence stars above 30–40  $M_{\odot}$ . Those less massive cannot lose all their hydrogen without the help of Roche lobe overflow. Hence, W-R Type Ib progenitors would have to be members of interacting binary systems. We emphasize that our models only assume a loss of the hydrogen envelope, not a mechanism for this loss.

*If Type Ib supernovae do originate in W-R stars, they account for the deaths of only the least massive ones. Why have we not seen the broad light curves of supernovae in larger W-R stars?* They would be intrinsically subluminal, though not much more so than SNIb (see models 14A, 14B, and 23A), unless less  $^{56}\text{Ni}$  is ejected because the proto-neutron star accretes additional matter while waiting for the delayed mechanism to produce the explosion. They could also have extra extinction due to recent envelope loss. More massive stars are rarer in general, and their supernovae would also be rarer than the present variety of SNIb, of which only a handful have been found. Perhaps there is a broad class of Type Ib supernovae waiting to be discovered.

Another possibility is that most W-R stars simply do not explode. Because of the greater ram pressure of infalling material and greater photodisintegration losses associated with a larger iron core, it is more difficult for the shock wave to

get out of the core and make more massive stars explode. If the neutrinos cannot rejuvenate a stalled shock (Wilson 1985), the whole star may collapse to form a black hole with no bright supernova explosion. This neglects rotation, which might allow such stars to produce supernova displays (Bodenheimer and Woosley 1983). Wheeler and Shields (1976) and Burrows (1987) argue that the black holes in X-ray binaries must come from  $10 M_{\odot}$  W-R- stars originally  $30\text{--}40 M_{\odot}$ . Accretion onto a neutron star would be too slow to produce a black hole of order  $10 M_{\odot}$  ( $7\text{--}15 M_{\odot}$ ), and the collapse of a  $10 M_{\odot}$  main-sequence star (no mass loss) is an unlikely source, since such stars are the easiest to disrupt, and statistics require that they produce neutron stars and supernovae. Galactic nucleosynthesis also implies that stars above some critical mass do not end as supernovae (Wheeler and Bash 1977; Twarog and Wheeler 1987).

## VI. CONCLUSIONS

The primary purpose of this paper was to address the issue of whether or not Type Ib supernovae come from massive stars that have lost their hydrogen envelopes before exploding. Given the current incomplete set of data—only one SNIb, SN 1983N, has a bolometric light curve, and that ends at a critical point—a definitive answer cannot be given at the present time. However, unless the light curve of SN 1983N proves to be atypical or in error, the massive-star models do have a serious flaw: their light curves are too flat. That is, the luminosity does not fall far enough from peak before beginning the exponential tail. The only solution to this problem is to invoke some mechanism that decreases the total deposition of radioactive decay energy (i.e., the average gamma-ray optical depth  $\kappa\rho r$ ) at an earlier time than strictly spherical hydrodynamics suggests. A possible mechanism might be clumping of the ejecta. Note, however, that the unusual event SN 1985F declined less after peak in the blue than did the other SNIb. If, as seems reasonable, its bolometric curve declined even less, then we can say that *it is possible that SN 1985F was the explosion of a Wolf-Rayet star.*

If (all or some) Type Ib supernovae do come from massive stars, our models set limits on the mass of the progenitor stars. The width of the light curves gives an upper bound of about  $5 M_{\odot}$  for the amount of material ejected (for reasonable explosion energies). This corresponds to a progenitor of  $6\text{--}7 M_{\odot}$ , the core of a star with a main-sequence mass of, at most, about  $25 M_{\odot}$ . Peak magnitudes imply a lower limit of  $\sim 2.5 M_{\odot}$  of ejecta and a  $15 M_{\odot}$  main-sequence star. The light curve of SN 1985F was somewhat broader than usual for SNIb, but it was not remarkably broad. It is unlikely that the presupernova star could have been over  $\sim 8 M_{\odot}$  at the time of the explosion, and it could very well have been only 5 or  $6 M_{\odot}$  (e.g., model 6A-b provides a credible, but nonunique, fit to the *estimated* light curve).

Stars in the allowed range are too small to lose all their hydrogen before core collapse without mass transfer; thus, if Type Ib progenitors are hydrogen-stripped stars, they are

probably members of interacting binary systems. The mass limits also imply that the identification of the progenitors with Wolf-Rayet stars, in particular, is probably incorrect. Only a small fraction of observed Wolf-Rayet stars were originally stars as small as  $20\text{--}25 M_{\odot}$ . It might be that the progenitors are the bared cores of massive stars, but not Wolf-Rayet stars per se (see, for instance, Uomoto and Kirshner 1986). Since most Wolf-Rayet stars are too massive to produce SNIb, their ultimate fate remains unknown. Their supernovae may simply be less numerous and more obscured than SNIb, implying that we have only to wait long enough to discover a slow variety of SNIb. On the other hand, they might eject very little  $^{56}\text{Ni}$ , or not explode at all but form black holes (Wheeler and Shields 1976; Burrows 1987).

Comparisons of SNIb and SNIa data show that the light curves of the two (except for SN 1985F) are nearly identical for the first few months, but the SNIa decline faster in the blue on the exponential tail. Although one really needs bolometric data to draw a clear conclusion, this implies that SNIa eject less matter and/or have larger expansion velocities. The amount of  $^{56}\text{Ni}$  ejected by the SNIb, as implied by the luminosity at the start of the tail ( $0.04\text{--}0.3 M_{\odot}$  for  $H_0 = 75$ ), is consistent, at the low end, with that ejected by the Type II supernovae SN 1987A (Woosley 1988) and SN 1980K (Uomoto and Kirshner 1986).

Independent of whether or not they explain SNIb, explosions of hydrogenless stars are of interest. We have calculated the bolometric light curves and composition and velocity profiles for a number of supernovae with massive progenitors which lost their hydrogen envelopes before core collapse. The main peak in the light curve is the result of the delayed escape of energy produced by the decay of  $^{56}\text{Ni}$  and  $^{56}\text{Co}$ . After peak, the supernova is powered directly by the radioactive decay of  $^{56}\text{Co}$ . A gamma-ray transport code (described in the Appendix) showed that an effective gamma-ray opacity of 0.03 or  $0.05 \text{ cm}^2 \text{ g}^{-1}$  would produce a more realistic tail slope than the  $0.07 \text{ cm}^2 \text{ g}^{-1}$  originally adopted.

While we are reluctant to give up the massive-star model for SNIb (the arguments given in various papers written before this study [see § IIb] still seem persuasive), it does have difficulty matching the bolometric light curve of SN 1983N. On the other hand, it may be able to explain SN 1985F. Perhaps there are two types of SNIb, only one of which, epitomized by SN 1985F, comes from hydrogen-stripped cores of massive stars. A more complete set of data, spectra, effects of circumstellar material, and other types of hydrogenless stars need to be considered further in the attempt to identify the origins of SN 1985F and Type Ib supernovae in general.

We would like to thank Phil Pinto and Rick Pogge for many useful discussions and invaluable assistance and advice. Thanks also to Tom Weaver for instructive conversations and permission to use the KEPLER code. This work has been supported by the National Science Foundation (AST-84-18185). Some of the calculations were carried out at the San Diego Supercomputer Center.

## APPENDIX

### GAMMA-RAY DEPOSITION

To calculate the late-time light curve, one must determine how much of the energy produced by decay is absorbed by the ejecta. KEPLER uses a simple prescription to convert the gamma rays and positron energy to bolometric luminosity. The optical depth to gamma rays from a zone at radius  $r$  to the surface is calculated assuming a constant effective gamma-ray opacity so  $\tau_r \equiv \kappa_r \int \rho dr$ .

There is no dependence on the ionization state, since the scattering cross section is independent of whether or not the electron is bound. A fraction,  $f_{\text{dep}} = (1 - e^{-\tau})$ , of the gamma-ray energy released within a zone is deposited into that same zone; the rest is assumed to escape the star completely as nonthermal gamma radiation. Actually, the energy produced in a zone should be spread over all those at larger radii, but the global transport of radiation is difficult to achieve in a locally coupled hydrodynamics code. The error should be acceptable for our purposes, especially when the optical depth is greater than a few. The positron kinetic energy is assumed to deposit completely at all times, since the cross sections for scattering off electrons and interacting with plasma modes are large and greater than that for annihilation until the positron has slowed substantially. Gamma rays produced by electron-positron annihilation are included with the primary gamma rays. Finally, the energy deposited within a zone is assumed to be converted by atomic processes into thermal blackbody radiation, which then diffuses out of the remnant.

This prescription was tested by recomputing some points on the tails of the models with a more detailed Monte Carlo gamma-ray transport code (Pinto, Axelrod, and Woosley 1988; Pinto 1988). The full spectrum of gamma-ray energies from  $^{56}\text{Co}$  decay was used, as well as Klein-Nishina cross sections and spherical geometry. The positron kinetic energy was always assumed to deposit *in situ*. Figure 9 shows the recomputed tails of models 8A and 6B with lines indicating the maximum and minimum luminosities possible. The maximum luminosity is given by the energy produced by the decay of  $^{56}\text{Co}$ , the minimum by the positron kinetic energy alone. All of the decay energy is depositing at the start of the tail. As time passes, the column depth of the ejecta decreases and more of the gamma rays (and X-rays from down-scattered gamma rays) escape.

The actual deposition of decay energy can be reproduced approximately by using average gamma-ray and positron energies and purely radial photon paths with a constant effective  $\kappa_\gamma$ , as is done in KEPLER. Weaver, Axelrod, and Woosley (1980) found that  $\kappa_\gamma = 0.07$  worked well for Type Ia supernovae, and we adopted that value. However, as shown in Figure 13, which compares some of KEPLER's tails to those from the Monte Carlo code, a smaller  $\kappa_\gamma$  would have been more realistic here. KEPLER must deposit less energy in the zones containing nickel to reproduce the total effect of depositing correct amounts of energy throughout the ejecta. Model 6B was rerun from shock breakout to 350 days with  $\kappa_\gamma = 0.03$ . The tail from this model (cf. Fig. 11) was a better match to that obtained from the Monte Carlo calculation.

Since the column depths are the same in the KEPLER and Monte Carlo runs, one can then surmise that 0.03 would have been better for model 6C also, and 0.05 for model 8A. Similarly, Colgate, Petschek, and Kriese (1980) and Sutherland and Wheeler (1984) found 0.03 (a local rather than global effective opacity, however) for constant-density models of SNIa. The value of 0.07 is too high, probably because increasing numbers of gamma-ray photons escape after only one or two collisions, carrying off energy which did not escape in the KEPLER runs. KEPLER assumes that all gamma rays which do not escape directly deposit all of their energy, but this is true only if they undergo many collisions before escaping the cloud. Using 0.03 rather than 0.07 affects only the tails of the light curves, while our primary conclusions are based on the earlier portion of the light curves. Thus, except for model 6B, the calculations were not repeated.

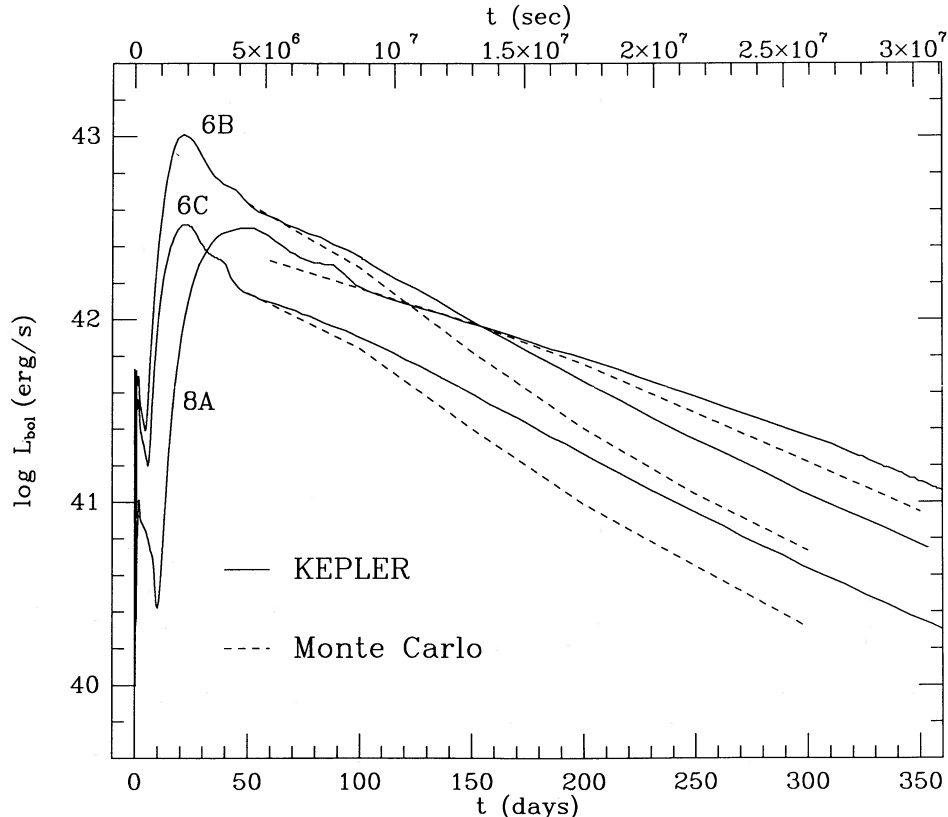


FIG. 13.—Light-curve tails calculated with a detailed Monte Carlo code compared with those calculated by the simple prescription in KEPLER using  $\kappa_\gamma = 0.07 \text{ cm}^2 \text{ g}^{-1}$ .

## REFERENCES

- Aaronson, M., Huchra, J., Mould, J., Schechter, P. L., and Tully, R. B. 1982, *Ap. J.*, **258**, 64.
- Abbott, D., Biegging, J. H., Churchwell, E., and Torres, A. 1986, *Ap. J.*, **303**, 239.
- Arnett, W. D. 1980, *Ap. J.*, **237**, 541.
- . 1983, *Ap. J.*, **253**, 785.
- Arnett, W. D., Branch, D., and Wheeler, J. C. 1985, *Nature*, **314**, 337.
- Axelrod, T. S. 1980, Ph.D. thesis, University of California, Santa Cruz. (Available as UCRL Preprint 52994 from Lawrence Livermore National Laboratory.)
- . 1988, in *IAU Colloquium 108, Atmospheric Diagnostics of Stellar Evolution*, ed. K. Nomoto (Dordrecht: Reidel), in press.
- Barbon, R., Ciatti, F., and Rosino, L. 1973, *Astr. Ap.*, **25**, 241.
- . 1979, *Astr. Ap.*, **72**, 287.
- . 1982, *Astr. Ap.*, **116**, 35.
- Begelman, M. C., and Sarazin, C. L. 1986, *Ap. J.*, **300**, 259.
- Bertola, F. 1964, *Ann. d'Ap.*, **27**, 319.
- Bertola, F., Mammano, A., and Perinotto, M. 1965, in *Contr. Asiago Obs.*, No. 174, p. 51.
- Blair, W. P., and Panagia, M. 1987, in *Exoloring the Universe with the IUE Satellite*, ed. Y. Kondo, W. Wamsteker, A. Boggess, M. Grewing, C. DeJager, A. L. Lane, J. L. Linsky, and R. Wilson (Dordrecht: Reidel), p. 549.
- Bodenheimer, P., and Woosley, S. E. 1983, *Ap. J.*, **269**, 281.
- Branch, D. 1986, *Ap. J. (Letters)*, **300**, L51.
- . 1988, in *IAU Colloquium 108, Atmospheric Diagnostics of Stellar Evolution*, ed. K. Nomoto (Dordrecht: Reidel), in press.
- Branch, D., and Bettis, C. 1978, *A.J.*, **83**, 224.
- Branch, D., Doggett, J. B., Nomoto, K., and Thielemann, F.-K. 1985, *Ap. J.*, **294**, 619.
- Branch, D., Lacy, C. H., McCall M. L., Sutherland, P. G., Uomoto, A., Wheeler, J. C., and Willis, B. J. 1983, *Ap. J.*, **270**, 123.
- Branch, D., and Nomoto, K. 1986, *Astr. Ap. Letters*, **164**, L13.
- Burrows, A. 1987, *Physics Today*, **40**, 28.
- Burstein, D., and Heiles, C. 1984, *Ap. J. Suppl.*, **54**, 33.
- Cahen, S., Schaeffer, R., and Casse, M. 1986, in *Nucleosynthesis and Its Implications on Nuclear and Particle Physics*, ed. J. Audouze and N. Mathieu (Dordrecht: Reidel), p. 243.
- Cameron, A. G. W., and Iben, I. 1986, *Ap. J.*, **305**, 228.
- Catchpole, R. M., et al. 1987, *M.N.R.A.S.*, **229**, 15P.
- Caughlan, G. R., Fowler, W. A., Harris, M. J., and Zimmerman, B. A. 1985, *Atomic Data Nucl. Data Tables*, **32**, 197.
- Chevalier, R. A. 1976, *Ap. J.*, **208**, 826.
- . 1984, *Ap. J. (Letters)*, **285**, L63.
- . 1986, in *Highlights Astr.* Vol. 7, ed. J. P. Swings (Dordrecht: Reidel), p. 599.
- Chiosi, C., and Maeder, A. 1986, *Ann. Rev. Astr. Ap.*, **24**, 329.
- Colgate, S. A., Petschek, A. G., and Kriese, J. T. 1980, *Ap. J. (Letters)*, **237**, L81.
- Conti, P. 1984, in *IAU Symposium 105, Observational Tests of the Stellar Evolution Theory*, ed. A. Maeder and A. Renzini (Boston: Reidel), p. 319.
- . 1986, in *IAU Symposium 116, Luminous Stars and Associations in Galaxies*, ed. C. W. H. de Loore, A. J. Willis, and P. Laskarides (Boston: Reidel), p. 199.
- de Loore, C. 1986, in *IAU Symposium 116, Luminous Stars and Associations in Galaxies*, ed. C. W. H. de Loore, A. J. Willis, and P. Laskarides (Boston: Reidel), p. 352.
- de Vaucouleurs, G. 1979, *A.J.*, **84**, 1270.
- Doggett, J. B., and Branch, D. 1985, *A.J.*, **90**, 2303.
- Elias, J. H., Matthews, K., Neugebauer, G., and Persson, S. E. 1985, *Ap. J.*, **296**, 379.
- Filippenko, A., Porter, A., Sargent, W., and Schneider, D. 1986, *A.J.*, **92**, 1341.
- Filippenko, A., and Sargent, W. 1985, *Nature*, **316**, 407.
- . 1986, *A.J.*, **91**, 691.
- Gaskell, C. M., Cappellaro, E., Dinerstein, H. L., Garnett, D., Harkness, R., and Wheeler, J. C. 1986, *Ap. J. (Letters)*, **306**, L77.
- Graham, J. R. 1986a, *M.N.R.A.S.*, **220**, 27P.
- . 1986b, *Ap. J.*, **315**, 588.
- Graham, J. R., Meikle, W. P. S., Allen, D. A., Longmore, A. J., and Williams, P. M. 1986, *M.N.R.A.S.*, **218**, 93.
- Harkness, R. P. 1987, in *Proc. 13th Texas Symposium on Relativistic Astrophysics*, ed. M. P. Ulmer (Singapore: World Scientific Publishing), p. 413.
- Harkness, R. P., et al. 1987, *Ap. J.*, **317**, 355.
- Iben, I., Nomoto, K., Tornambè, A., and Tutukov, A. 1987, *Ap. J.*, **317**, 717.
- Khokhlov, A. M., and Ergma, E. V. 1986, *Soviet Astr. Letters*, **12** (No. 3), 152.
- Maeder, A. 1984, in *IAU Symposium 105, Observational Tests of the Stellar Evolution Theory*, ed. A. Maeder and A. Renzini (Boston: Reidel), p. 319.
- . 1987, *Astr. Ap.*, **173**, 247.
- Maeder, A., and Lequeux, J. 1982, *Astr. Ap.*, **114**, 409.
- Maeder, A., and Meynet, G. 1987, *Astr. Ap.*, **182**, 243.
- Massey, P. 1982, in *IAU Symposium 99, Wolf-Rayet Stars: Observations, Physics, Evolution*, ed. C. de Loore and A. J. Willis (Boston: Reidel), p. 251.
- Mayle, R., and Wilson, J. R. 1987, *Ap. J.*, submitted.
- Minkowski, R. 1941, *Pub. A.S.P.*, **53**, 224.
- Panagia, N. 1987, in *High Energy Phenomena around Collapsed Stars*, ed. F. Pacini (Boston: Reidel), p. 33.
- Panagia, N., Sramek, R. A., and Weiler, K. W. 1986, *Ap. J. (Letters)*, **300**, L55.
- Pinto, P. 1988, Ph.D. thesis, University of California, Santa Cruz.
- Pinto, P., Axelrod, T., and Woosley, S. 1988, in preparation (Paper II).
- Porter, A., and Filippenko, A. 1987, *A.J.*, **93**, 1372.
- Richter, O.-G., and Rosa, M. 1984, *Astr. Ap. Letters*, **140**, L1.
- Richtler, T., and Sadler, E. M. 1983, *Astr. Ap. Letters*, **128**, L3.
- Sandage, A., and Tammann, G. A. 1981, *Revised Shapley-Ames Catalog of Bright Galaxies* (Washington, D.C. Carnegie Institution of Washington).
- . 1982, *Ap. J.*, **256**, 339.
- Schaeffer, R., Casse, M., and Cahen, S. 1987, *Ap. J. (Letters)*, **316**, L31.
- Schild, H. 1986, in *IAU Symposium 116, Luminous Stars and Associations in Galaxies*, ed. C. de Loore, A. J. Willis, and P. Laskarides (Boston: Reidel), p. 423.
- Schurmann, S. R. 1983, *Ap. J.*, **267**, 779.
- Sramek, R. A., Panagia, N., and Weiler, K. W. 1984, *Ap. J. (Letters)*, **285**, L59.
- Sutherland, P., and Wheeler, J. C. 1984, *Ap. J.*, **280**, 282.
- Tammann, G. A. 1982, in *Supernovae: A Survey of Current Research*, ed. M. J. Rees and R. J. Stoneham (Dordrecht: Reidel), p. 371.
- Tsvetkov, D. Y. 1985, *Soviet Astr.*, **29** (No. 2), 211.
- . 1986, *Soviet Astr. Letters*, **12** (No. 5), 328.
- Twarog, B. A., and Wheeler, J. C. 1987, *Ap. J.*, **316**, 153.
- Uomoto, A. 1986, *Ap. J. (Letters)*, **310**, L35.
- Uomoto, A., and Kirshner, R. P. 1985, *Astr. Ap. Letters*, **149**, L7.
- . 1986, *Ap. J.*, **308**, 685.
- Weaver, T. A., Axelrod, T. S., and Woosley, S. E. 1980, in *Type I Supernovae*, ed. J. C. Wheeler (Austin: University of Texas), p. 113.
- Weaver, T. A., Woosley, S. E., and Fuller, G. M. 1985, in *Numerical Astrophysics* ed. J. Centrella, J. LeBlanc, and R. Bowers, (Boston: Jones & Bartlett), p. 374.
- Weaver, T. A., Zimmerman, G. B., and Woosley, S. E. 1978, *Ap. J.*, **225**, 1021.
- Weiler, K. W., Sramek, R. A., Panagia, N., van der Hulst, J. M., and Salavati, M. 1986, *Ap. J.*, **301**, 790.
- Wheeler, J. C., and Bash, F. N. 1977, *Nature*, **268**, 706.
- Wheeler, J. C., and Harkness, R. P. 1986, in *NATO Advanced Research Workshop on Galaxy Distances and Deviations from Universal Expansion* (Kona, Hawaii), ed. B. Madore and R. B. Tully (Boston: Reidel), p. 45.
- Wheeler, J. C., Harkness, R. P., Barkat, Z., and Swartz, D. 1986, *Pub. A.S.P.*, **98**, 1018.
- Wheeler, J. C., Harkness, R. P., and Cappellaro, E. 1987, in *Proc. 13th Texas Symposium on Relativistic Astrophysics*, ed. M. P. Ulmer (Singapore: World Scientific Publishing), p. 402.
- Wheeler, J. C., and Leveault, R. 1985, *Ap. J. (Letters)*, **294**, L17.
- Wheeler, J. C., and Shields, G. A. 1976, *Nature*, **259**, 642.
- Wilson, J. R. 1985, in *Numerical Astrophysics*, ed. J. Centrella, J. LeBlanc, and R. Bowers (Boston: Jones & Bartlett), p. 422.
- Willson, J. R., Mayle, R., Woosley, S. E., and Weaver, T. A. 1986, in *Proc. 12th Texas Symposium on Relativistic Astrophysics*, ed. M. Livio and G. Shaviv (New York: New York Academy of Sciences), p. 267.
- Woosley, S. E. 1986, in *Nucleosynthesis and Chemical Evolution*, ed. J. Audouze, C. Chiosi, and S. E. Woosley, (Geneva: Geneva Observatory), p. 129.
- . 1988, *Ap. J.*, **330**, 218.
- Woosley, S. E., Pinto, P., and Ensmann, L. 1988, *Ap. J.*, **324**, 466.
- Woosley, S. E., and Weaver, T. A. 1986, *Ann. Rev. Astr. Ap.*, **24**, 205.
- . 1988, in preparation (Paper II).

*Note added in proof.*—Tsvetkov (*Soviet Astr. Letters*, **13** [No. 5], 376 [1987]) and Harkness et al. (*Ap. J.*, **317**, 355 [1987]) have provided *B* and *V* data for SN 1984L (photographic photometry and integrated spectra, respectively). The *B*-band data can be fitted to either SN 1985F or SN 1964L, depending on whether 1984L was discovered  $\sim 2$  or  $\sim 10$  days after peak, but in both cases, the *V*-magnitude light curve is flatter than usual (cf. Fig. 1). Assuming that the bolometric magnitude follows *V*, the bolometric light curve of 1984L lies between that of 1983N and the estimated bolometric light curve of 1985F. Hence, there is a possibility that the progenitor of SN 1984L was also a 6–8  $M_{\odot}$  W-R star. A modest amount of clumping may still be necessary; the data are not clear enough to more definite.

LISA ENSMAN and STANFORD E. WOOSLEY: Board of Studies in Astronomy and Astrophysics, Lick Observatory, University of California, Santa Cruz, CA 95064